University of Denver

Digital Commons @ DU

8-2023

Hemodynamic Assessment of Y-Incision Aortic Root Enlargement Using Computational Simulations

Astitwa Ghimire
University of Denver

Follow this and additional works at: https://digitalcommons.du.edu/etd

Part of the Biomechanical Engineering Commons, Biomedical Devices and Instrumentation Commons, and the Other Biomedical Engineering and Bioengineering Commons

Hemodynamic Assessment of Y-Incision Aortic Root Enlargement Using Computational Simulations

Abstract

The Yang procedure is a new aortic root enlargement technique used to enlarge the aortic annulus by multiple valve sizes. The procedure prevents patient prosthesis mismatch and establishes a viable platform for future valve-in-valve implantation. This study used the Yang procedure to investigate the hemodynamics in the aortic root and bioprosthetic valve regions after aortic root enlargement. Results indicate the velocity magnitude at the sinus regions of a patient who underwent the Yang procedure was slower, indicating risks of flow stasis and thrombosis. Simulation results denote computational models can be created for optimization of surgical procedures.

Document Type

Masters Thesis

Degree Name

M.S.

First Advisor

Ali Azadani

Second Advisor

Matt Gordon

Third Advisor

Yan Qin

Keywords

Aortic root enlargement, Valve-in-valve implantation, Yang procedure, Hemodynamics

Subject Categories

Biomechanical Engineering | Biomedical Devices and Instrumentation | Biomedical Engineering and Bioengineering | Engineering | Mechanical Engineering | Other Biomedical Engineering and Bioengineering

Publication Statement

Hemodynamic Assessment of Y-incision Aortic Root Enlargement Using Computational
Simulations

_____

A Thesis

Presented to

the Faculty of the Daniel Felix Ritchie School of Engineering and Computer

Science

University of Denver

_____

In Partial Fulfillment

of the Requirements for the Degree

Master of Science

_____

by

Astitwa Ghimire

August 2023

Advisor: Ali Azadani

Author: Astitwa Ghimire
Title: Hemodynamic Assessment of Y-incision Aortic Root Enlargement Using Computational Simulations
Advisor: Ali Azadani
Degree Date: August 2023

Abstract

The Yang procedure is a new aortic root enlargement technique used to enlarge the aortic annulus by multiple valve sizes. The procedure prevents patient prosthesis mismatch and establishes a viable platform for future valve-in-valve implantation. This study used the Yang procedure to investigate the hemodynamics in the aortic root and bioprosthetic valve regions after aortic root enlargement. Results indicate the velocity magnitude at the sinus regions of a patient who underwent the Yang procedure was slower, indicating risks of flow stasis and thrombosis. Simulation results denote computational models can be created for optimization of surgical procedures.

Acknowledgments

I would like to express my heartfelt gratitude to my advisor, Dr. Azadani, for their unwavering support, invaluable guidance, and immense patience throughout the journey of my master's thesis. Their expertise, encouragement, and constructive feedback have been instrumental in shaping the outcome of this research.

I am deeply thankful to Dr. Yang from the University of Michigan for providing the deidentified computed tomography angiography data of patients and to the University of Denver for providing me with the remarkable opportunity to pursue my master's degree. The academic environment and resources have been pivotal in fostering my intellectual growth and nurturing my passion for research.

Table of Contents

List of Figures

Chapter 1: Introduction

The Heart

The heart is divided into two sections, and both sections function as pumps in series (Figure 1-1). The high-pressure systemic pump is located on the left side and is composed of the left ventricle and left atrium. The low-pressure pulmonary pump is situated on the right side and is devised of the right ventricle and atrium. The left ventricle's outflow tract connects to the aortic root. The aortic valve is located at the junction of the two. To support greater hemodynamic pressure, the left ventricle wall is three times thicker than the right ventricle [1].

Four cardiac valves lie almost vertically behind the sternum. Valve locations from above downwards are the pulmonary valve (PV), aortic valve (AV), mitral valve (MV), and tricuspid valve (TV). The PV separates the right ventricle and pulmonary artery, the AV separates the left ventricle and aorta, the MV separates the left atrium and left ventricle, and the TV separates the right atrium and right ventricle [2]. The valves are divided into semilunar (PV and AV) and atrio-ventricular (TV and MV) [3]. To avoid retrograde flow back into ventricles during the diastolic cycle, semilunar valves, which have three leaflets and resemble a nearly round disc, are used. During the systolic cycle, atrio-ventricular valves prohibit backwards flow from the ventricle to the atrium. The MV

is made of two leaflets, while the TV has leaflets of three different sizes. The biomechanics of the heart can be described by tension, shear, and flexure. The loading modes are applied cyclically as the valves open (flexure), allow blood to pass (shear), close (flexure), and prevent reverse blood flow.

Blood flow returning from the body to the lungs for oxygenation is modulated by the PV and TV on the right side of the heart [4]. Oxygenated blood flow to the body is controlled by the MV and AV on the left side of the heart. The PV and AV, respectively, permit blood to flow from the ventricles into the right and left coronary arteries. In the right and left sides of the heart, the AV and MV allow blood to circulate between the atria and ventricles, respectively. Blood is supplied from the left and right coronary arteries in the heart. The coronary arteries are the first branches of the aorta, originating from the aortic root. There are three aortic sinuses (sinuses of Valsalva), which are present above each cusp of the aortic valve. The left and right coronary arteries are given rise by the left and right aortic sinuses. In the systolic and diastolic cycles, the AV and PV open when the ventricle contracts and close when it relaxes, filling the ventricles through the MV and TV [3, 4].
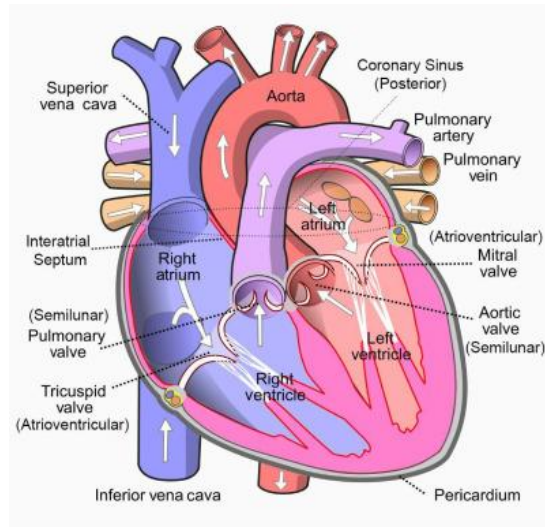
Figure 1-1: Blood circulation through the heart [5].

Aortic Stenosis

In the United States, aortic stenosis (AS) is a prevalent valvular heart disease often occurring in the elderly (~75 years of age) due to an active inflammatory process [6]. Inflammation brought on by hemodynamic stresses results in lipid infiltration and leaflet immobility in the aortic valve because of ongoing calcification. Unless mechanical restriction to the left ventricular outflow is removed by replacing the aortic valve, the life expectancy of a person with AS is approximately three years once symptoms have emerged. In adults with calcified aortic valves, valve replacement is suggested, as patients with valve replacements are expected to achieve age rates standard in the population [7].

The two main causes of AS are as follows: one to two percent of the population is born with a bicuspid aortic valve, which increases stenosis susceptibility, and AS develops with age [7]. In AS, the outflow is obstructed due to the decrease in the functional area of the aortic valve. Hemodynamics are negligibly affected when the

3

normal 3 to 4 cm^2 area of the aortic valve is reduced by half. The left ventricle undergoes

a progressive pressure overload when the aortic valve area is reduced to 1/4th of its

normal size, causing severe flow obstruction. Maladaptive and adaptive concentric

hypertrophy develops in the left ventricle in response to the overload. The left ventricle

can produce the force necessary to push the blood past the obstruction, attributable to the

greater muscular mass. However, the enlarged myocardium has a reduced coronary blood

flow reserve and may cause systolic and diastolic left ventricular dysfunction. These

factors produce symptoms of congestive heart failure.

Small Aortic Annuli in Patients

Leaflet calcification and thickening are symptoms of valvular AS, which causes

poor exercise tolerance, reduced cardiac output, heart failure, and mortality [8].

Hemodynamics, symptoms, valvular anatomy, and the effects on the function of the left

ventricle characterize the severity of the disease. Aortic valve replacement (AVR) is the

recommended method of treatment for severe aortic stenosis. To achieve mass regression,

AVR attempts to minimize left ventricular pressure and volume overload. AVR drastically

improves survival in patients with symptomatic severe AS [9]. For success, the

transvalvular gradient following surgery should be nominal [8]. High-gradient AS is

denoted as aortic valve area (AVA) ≤ 1 cm^2 with a maximum aortic jet velocity ≥ 4 m/s or

a mean transvalvular pressure gradient ≥ 40 mmHg. Some indications for AVR include (1)

high-gradient AS with symptoms, (2) moderate AS in patients who are undergoing non-

AS related cardiac surgery, and (3) severe AS in symptomless patients, low surgical risk, and fast disease progression.

In AVR, a small aortic annulus (SAA) poses significant problems. SAA is defined as an aortic annulus of ≤ 21 mm, incapable of accommodating a prosthetic bigger than this size. SAA can also be identified as the aortic sinotubular diameter indexed for height, with less than 1.5 cm/m cutoffs in males and less than 1.4 cm/m in females [10]. 88% - 91% of female patients receive a smaller prosthesis [8], and the occurrence of patients receiving a small prosthesis varies from 22% to 44%. Patients with SAA display higher surgical risk profiles [11]. Patient prosthesis mismatch (PPM) is a concern occurring postoperatively after AVR in a small aortic annulus. PPM occurs when the effective orifice area (EOA) of the valve prosthesis is too small for the patient's body. Insufficient cardiac output and functional aortic stenosis result from PPM. The accepted threshold from PPM is 0.85 cm^2/m^2, and a value less than 0.65 cm^2/m^2 is deemed severe. Implications of PPM include structural valve deterioration, an independent predictor of long-term mortality, and a higher transvalvular gradient, preventing left ventricle mass regression.

Mechanical and Bioprosthetic Heart Valves

AVR uses artificial tissue-engineered, bioprosthetic (Figure 1-2) and mechanical (Figure 1-3) heart valves [12]. Tissue from animals or animal valves are used to produce bioprosthetic valves. Mechanical valves are often comprised of pyrolytic carbon and metal alloys [13]. In-vitro production of tissue-engineered valves involves the seeding of

human cells onto scaffolds. Bioprosthetic valves are recommended for individuals 70

years of age or older, at high risk of complications from anticoagulation, or those with

contraindications to anticoagulants [12]. Mechanical valves are recommended for patients

younger than 50 years of age with low risk of long-term anticoagulation, no

contraindications, intervention is high-risk, or if anticoagulants are used to treat another

condition.
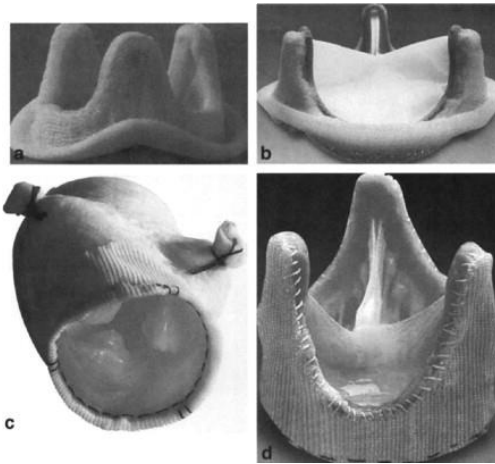
Figure 1-2: Xenograft tissue valves. (A) The Medtronic Hancock Bioprosthesis. (B) The Baxter Perimount (Registered trademark, Edwards LLC) valve. (C) The Medtronic Freestyle stentless xenograft. (D) The St. Jude Toronto SPV (registered trademark of St. Jude Medica [14].
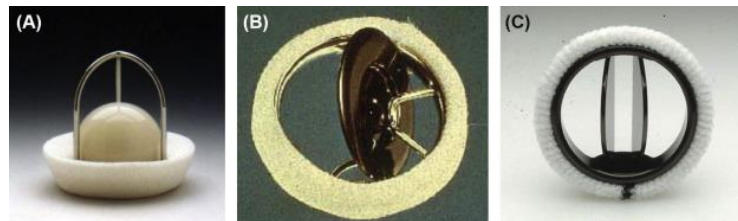
Figure 1-3: Mechanical prosthetic heart valves. (A) Starr-Edwards caged-ball valve. (B) Bjork-Shiley tilting disk valve. (C) St. Jude Medical bi-leaflet tilting disk heart valve [15].

There are three types of mechanical valves: caged ball valves, tilting disk valves,

and bi-leaflet valves. The most common mechanical prosthesis, the bi-leaflet

valve, has two semicircular leaflets and is reported to be the least thrombogenic of all

mechanical valve types. Although mechanical heart valves are renowned for their longevity of up to 20 years, they may additionally increase the risk of blood clotting and cause mechanical hemolytic anemia. When compared to bioprosthetic valves, mechanical valves are more prone to bleeding issues (1% to 2% vs. 0.7%) due to the long-term anticoagulation requirements to prevent thromboembolic risks. Endocarditis, ring abscess, and paravalvular leakages are other known complications.

Three bioprosthetic valve types are available: xenografts, homografts, and autografts, with xenografts being the most available [13]. Bioprosthetic valves do not require anticoagulants and exhibit excellent hemodynamic properties, similar to native valves. However, structural valve degeneration (SVD) limits the longevity of bioprosthetic valves, and treatment of SVD will require redoing valve replacement. The lifespan of bioprosthetic valves is directly correlated to the durability of the chemically cross-linked extracellular matrix. Mechanical stresses (bending deformations, shear, and leaflet tension), dystrophic calcification, and immune rejection are other factors leading to the degeneration of bioprosthetic valves.

Transcatheter and Surgical Aortic Valve Replacement

Surgical Aortic Valves

Heart-lung machines function to halt the heart and grant access to the aortic valve during surgical aortic valve replacement (SAVR) [16]. Median sternotomy has been the traditional approach to allow access to the heart. Mechanical or bioprosthetic valves can be used in SAVR, but stented bioprosthetic valves are more commonly used [8].

Decreased EOAs and increased transvalvular gradients are observed in bioprosthetic valves with a stent and sewing ring. In patients with SAA, this increases the occurrence of PPM. Stentless valves provide larger EOAs in patients due to the absence of the sewing ring and stent. Stentless valves aim to mimic the native anatomy of the aortic valve and result in superior clinical outcomes and hemodynamics; a longer cardiopulmonary bypass time is typically required, and technical challenges must be considered [17]. Stentless valves can be implanted using root or subcoronary techniques [8]. Full root or root inclusion techniques are preferred in patients with SAA. A larger valve can be inserted with full root replacement, improving the EOA, reestablishing the function of the Valsalva sinus, strengthening sinotubular function, and reducing the risk of PPM [18-20].

Transcatheter Aortic Valves

A minimally invasive procedure, known as transcatheter aortic valve replacement (TAVR) (Figures 1-4 and 1-5), is used to treat valve stenosis in individuals who are deemed high-risk for valve replacement using open heart surgery (Figure 1-6) [21]. To restore native valve function, a transcatheter aortic valve (TAV) can be inserted into a patient's diseased aortic valve using fluoroscopy. TAVs can be self- or balloon-expandable and are placed against the permanently opened calcified native leaflets of the patient. The stent is held in place by radial force. Previously implanted ineffective transcatheter or bioprosthetic valves can also be replaced with TAVs, a procedure known as valve-in-valve (ViV). The foldable stent frame retaining valve leaflets and the absence of a sewing cuff are notable features of TAVs.
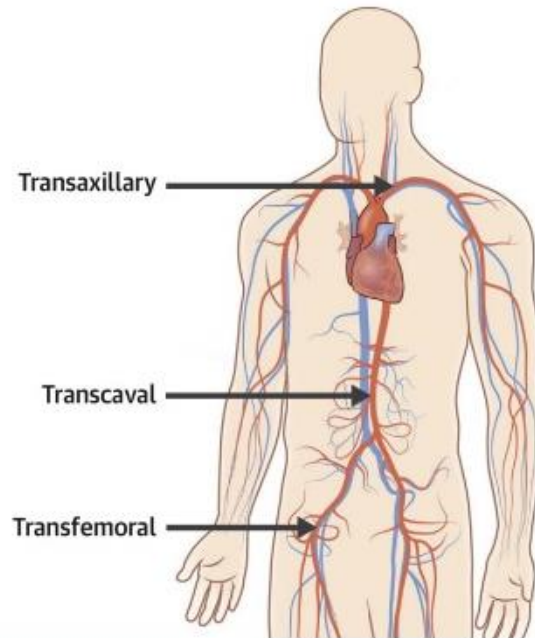
Figure 1-4: Entry points of a microcatheter for patients undergoing TAVR [22].

Figure 1-5: An illustration showcasing TAVR [23].
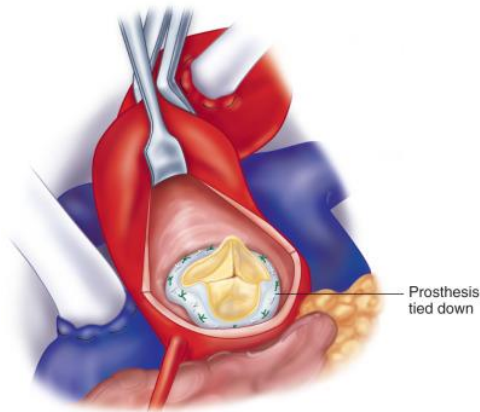
Figure 1-6: Valve implantation using SAVR [24].

TAVR is appealing because of its less invasive nature but suffers from complications developing in patients postoperatively. Common complications include thrombosis, PPM, mispositioning, and leaflet damage due to crimping. Postoperative complications are challenging to predict but may be influenced by patient-specific risk factors such as calcification of the native valve, mechanical and geometric properties of the aortic root, and various heart diseases.

Leon del Pino et al. [25] studied patients undergoing TAVR and discovered 25% of individuals developed PPM. PPM was linked to smaller prosthesis size and SAA. SAA and severe AS in elderly patients were investigated in another study, and results indicate TAVR provided favorable hemodynamic outcomes [26]. Severe PPM rates were 6% in both studies.

The outcomes of stented and stentless valves have been examined in numerous studies. Most studies demonstrate patients with stentless valves have much lower peak and mean transvalvular gradients and larger EOAs, which reduces left ventricle end-diastolic diameter and promotes mass regression [27, 28].

Patients with SAA have been studied to compare the outcomes of SAVR and TAVR [29, 30]. A larger EOA, lower rate of severe PPM, and a lower mean gradient was observed in patients who received TAVR when compared to SAVR patients. There was no difference between SAVR and TAVR among patients with SAA, however, a decreased mean gradient was observed after TAVR [31].

Valve-in-Valve Aortic Implantation

In the United States, about 5% of TAVR procedures are ViV TAVR (Figure 1-7) [32]. Bioprosthetic valves are being used instead of mechanical valves due to their hemodynamic properties and elimination of anticoagulant requirements. However, structural valve deterioration is common in bioprosthetic valves, occurring approximately 5-7 years after SAVR [33]. Replacement of bioprosthetic valves can be accomplished using the ViV technique. The minimally invasive percutaneous procedure allows a valve to be implanted directly within a failing bioprosthetic valve [34].
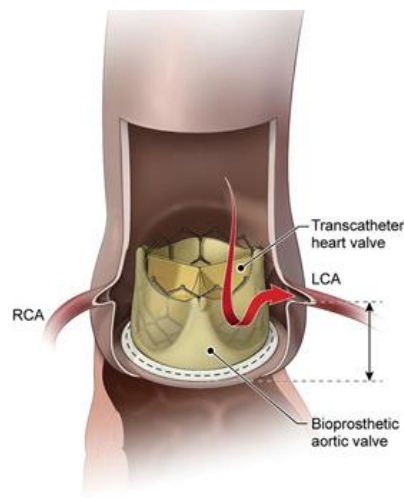
Figure 1-7: An illustration showcasing ViV TAVR for stented bioprosthetic aortic valves [35].

The Global Valve-In-Valve Registry of 202 patients indicated that procedural success was 93.1%, 84.1% of patients displayed improved function, and 58.9% exhibited elevated postprocedural gradients. High postprocedural gradients were observed in 28.4% of patients due to reduced EOA, device malposition in 15.3%, and a mortality rate of 8.4% in all cases. Data from systematic reviews show ViV TAVR had a higher incidence of severe PPM, myocardial infarction, and major bleeding when compared to redo-SAVR [36]. Nonetheless, a lower incidence of postoperative complications and lower mortality rates were noted.

A limitation of ViV TAVR is PPM, often seen in small bioprosthetic surgical valves [37]. PPM issues arise due to reduced EOA after ViV TAVR since the transcatheter heart valve is implanted in the stented ring of the existing bioprosthetic valve. Small bioprosthetic valve sizes (≤21 mm) are often associated with PPM due to reduced EOA in patients, causing reduced hemodynamics in patients [38]. A study with 79 patients undergoing ViV identified 61% of patients experienced suboptimal valve hemodynamics (at least moderate aortic regurgitation and/or a residual aortic mean gradient of ≥20 mm Hg) after ViV compared to early post-SAVR. Following ViV, pre-existing bioprosthetic failure and PPM due to stenosis were independently associated with a high residual gradient. Patients with existing PPM or bioprosthetic stenosis exhibited higher hemodynamic futility (18.5%) than those without PPM or bioprosthetic stenosis (7.6%). After ViV, hemodynamic levels were restored to early-post SAVR levels in only 1/3rd of patients.

According to a VIVID registry study on ViV TAVR, 32% of patients developed severe PPM after the procedure, which was associated with higher long-term mortality after TAVR and SAVR [37]. Furthermore, an inverse association between 1-year mortality and surgical valve size was identified. The PARTNER 2 Valve-in-Valve registry concluded patients with higher residual postprocedural gradients ($\geq$20 mmHg) after ViV TAVR had a higher 1-year mortality rate of 16.7% when compared to patients with a gradient <20 mmHg (7.7%). These findings indicate the importance of maximizing the EOA in patients with small aortic annuli to reduce PPM due to small bioprosthetic valve sizes.

Aortic Root Enlargement

Aortic root enlargement (ARE) is a procedure used to aid in implanting prosthetic valves in patients undergoing AVR [39]. Without ARE, patients may require the implantation of a smaller prosthesis due to a SAA, leading to complications. The earliest ARE technique was the Nicks procedure, enabling treatment of small aortic annuli by extending the aortotomy via the noncoronary sinus and inserting a patch to enlarge the annulus [40]. The Nicks procedure lessens the likelihood of PPM and enables the placement of a larger valve [39]. The Manouguian technique was developed in 1979 [41]. The procedure involves incising through the aorta and creating a larger diameter in the annulus, allowing the placement of a larger valve.

Studies have shown a higher indexed EOA in patient groups undergoing ARE before AVR compared to patients undergoing AVR only [42]. Yu et al. further supports

these conclusions, claiming ARE reduces the occurrence of PPM [43]. These studies

indicate ARE is often successful, allowing larger prosthetic implantation and reducing the

risk of PPM. However, another study using 4120 patients indicated patients who

underwent AVR with ARE experienced a higher rate of postoperative respiratory failure

than those who received AVR without ARE [44]. Other literature has not supported the

finding, but respiratory failure was identified as an independent risk factor. Most

literature has indicated ARE as a safe adjunct to AVR, and there is uncertainty regarding

whether there are any disadvantages to performing ARE [39].

Surgical Procedures

Cardiothoracic surgeons use the Manouguian [41] and Nicks [40] procedures to

enlarge aortic roots in patients with SAA (Figure 1-8). Following the Manouguian

procedure includes a risk of mitral regurgitation and requires incising the left atrium (LA)

and mitral valve (MV) anterior leaflet. Patients typically see a valve size increase of one

to two. The Nicks procedure usually increases the aortic annulus by one valve size by

making a vertical incision through the commissure. The incision is carried between the

left coronary cusp and noncoronary cusp to the inner leaflet triangle [45, 46].
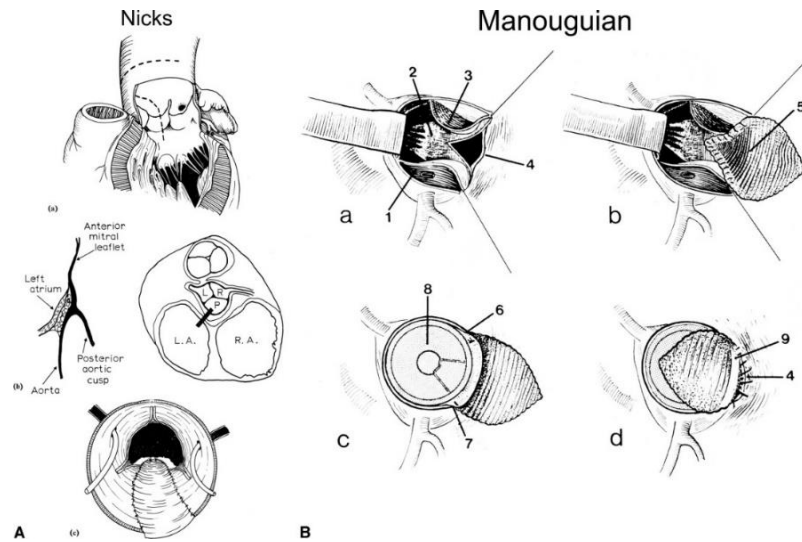
Figure 1-8: Figures from articles published by Nicks and colleagues (A) and Manouguian and Seybold-Epting (B) first describing posterior root enlargement techniques [47].

A new surgical technique deemed the Yang Procedure [46], enlarges the aortic annulus by two to five valve sizes without violation of the MV or LA [48-50] to prepare patients for future ViV TAVR and prevent PPM (Figure 1-9). From August 2020 to February 2022, Yang and colleagues reported 50 cases of AVR using the Yang and other cardiac procedures to primarily treat severe AS [51]. The native aortic annular size was 21 (19, 23) mm. After ARE, the median prosthesis size was 27 (27, 29) mm, with 54% of patients having the largest-sized valve or a size 29. Postoperative computed tomography aortogram after three months showed aortic root enlargement from 27 (24, 30) to 40 (36, 41) mm without aortic pseudoaneurysm. In another case, a patient with a small aortic annulus and root (≤17 mm) underwent ARE, enlarging the aortic annulus by five valve sizes (from 16 to 17 mm to 27 mm) and enlarging the sinotubular junction and proximal ascending aorta for future ViV TAVR using the Yang procedure [50].

15

The fibrous portion of the aortic root is enlarged by replacing the aortomitral curtain with a rectangular patch to accommodate valve size upscaling. Sewing the patch to the aortic and mitral annuli provides more stability when compared to the Manouguian and Nicks procedures, which sew the patch to the aortomitral curtain. It can be difficult to differentiate the mitral annulus, MV, and aortomitral curtain during surgery. Therefore, a "Y" incision is used in the Yang procedure instead of a "T" incision to avoid accidental incisions of the MV or LA. Without dissection of the aortic root, the "Y" incision can be extended to the nadirs of the aortic annulus from the aortomitral curtain. Passing the fibrous tissue under the nadirs of both left noncoronary sinuses may result in the rectangular patch pushing on the left coronary sinus and disruption of the left coronary artery. The rectangular patch is placed in front of the transverse sinus, allowing the left coronary sinus and patch to expand posteriorly without significantly disrupting the left coronary artery. Therefore, sizes larger than the rectangular patch should not be used.
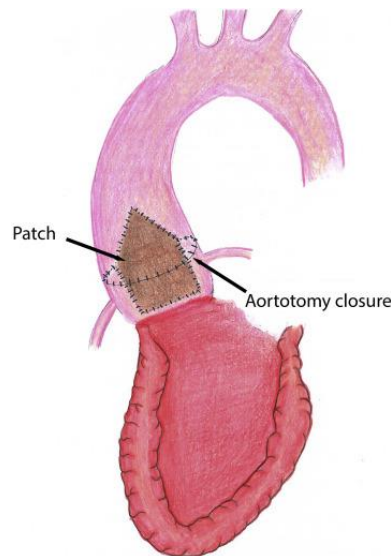
Figure 1-9: Illustration of the Yang procedure using the rectangular patch after Y-incision through the aorto-mitral curtain and closure of the aortotomy [52].

16

Chapter 2: Materials and Methods

Patient Data and Geometry Modeling

Two patient-specific anatomy models were constructed using computed tomographic angiography (CTA) images. Patient 1 underwent the Y-incision aortic root enlargement procedure and had a 27 mm Carpentier-Edwards PERIMOUNT Magna Ease valve sewed into the aortic root. Postoperative computed tomography angiograms were collected after three months. Computational fluid dynamic simulations were designed to investigate blood flow dynamics after aortic root enlargement. Blood flow patterns, including wall shear stress, pressure, and velocity, were quantified in the aortic root and near the bioprosthetic heart valve. The blood flow characteristics were compared to a control subject (Patient 2) who did not undergo the Y-incision aortic root enlargement procedure and received a 25 mm Carpentier-Edwards PERIMOUNT Magna Ease valve.

Patient CTA data was imported into Materialise Mimics 19.0 and the 3D aortic root and valve geometries were extracted (Figure 2-1). The valve geometries were exported to Geomagic Design X 2020 and SolidWorks Student Edition 2022, and simplified valve geometries were created using the original models as references (Figure 2-2). The aortic geometries were exported to Geomagic Design X, modified, smoothed, trimmed, and mated with the adapted valve geometries from SolidWorks. The aortic-

valve geometries were lofted together in SolidWorks to replicate simplified native aortic

root anatomy with valve implantation (Figure 2-3).
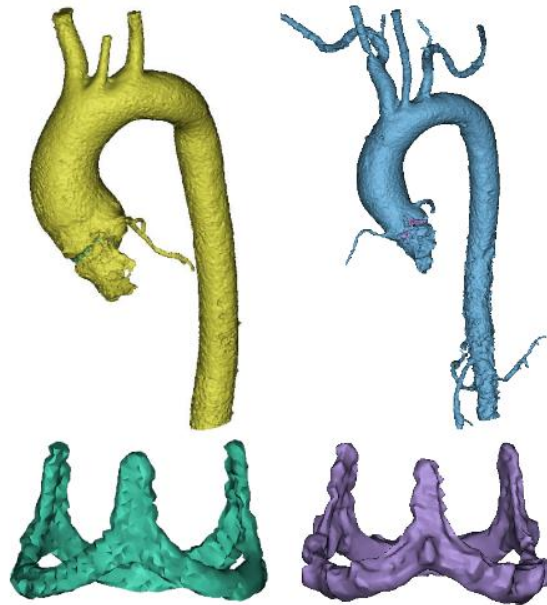
Figure 2-1: 3D geometries extracted from Materialise Mimics for patient 1 (left) and patient 2 (right).
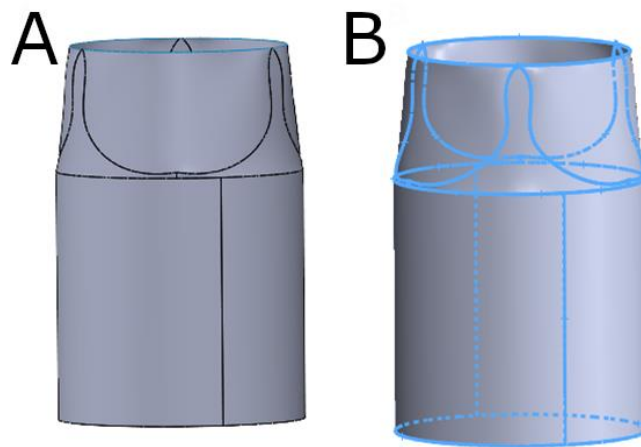
Figure 2-2: Simplified valve geometries created for patient 1 (A) and patient 2 (B) in SolidWorks.
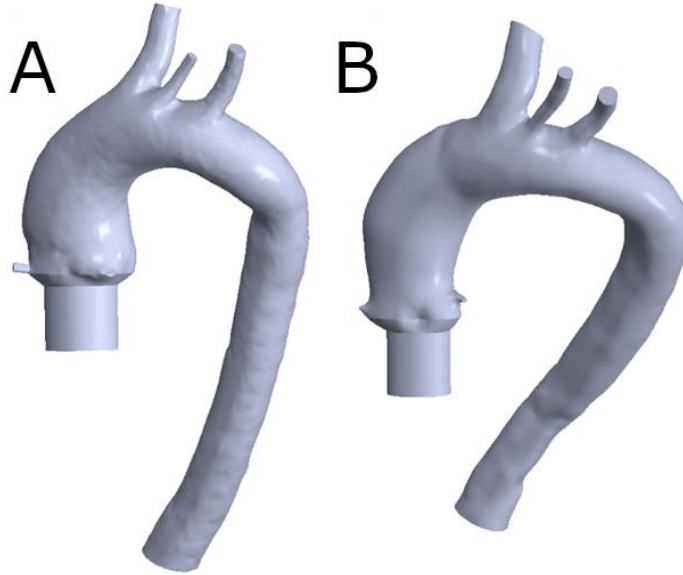
Figure 2-3: Modified native aortic root geometries of patient 1 (A) and patient 2 (B) with simplified bioprosthetic valves created in SolidWorks.

The aortic-valve models were meshed in PointWise 18.1 (Figure 2-4). Five different meshes were created for each model (Table 1). Mesh refinement was conducted to ensure an absence of mesh dependency for simulations.
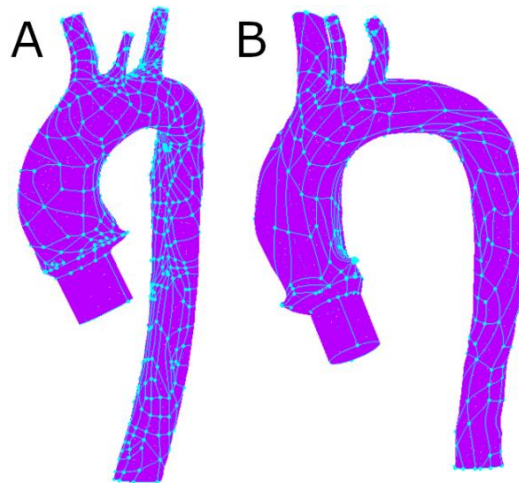
Figure 2-4: Aortic-valve geometries reconstructed in Pointwise for patient 1 (A) and patient 2 (B).

Mesh Grade	Patient 1 Element Count	Patient 2 Element Count
Coarse	2,244,726	3,211,050
Semi-Coarse	4,819,577	5,873,913
Medium	7,938,249	9,692,709
Semi-Fine	10,946,797	12,085,832
Fine	12,901,279	16,362,904

Table 1: Element counts of mesh used in computational fluid dynamic simulations for patient 1 and patient 2 to ensure mesh independence.

The Navier-Stokes equations were used to describe the flow conditions, which were considered to be steady-state and laminar. Blood was simulated as a Newtonian viscous fluid with a constant viscosity of 0.00408 Pa.s, incompressible, homogenous, and isotropic with a density of 1060 kg/m^3. Walls of the vessel are assumed rigid with no-slip conditions. Two different boundary conditions were applied. Mass flow rate was calculated using the cross-sectional area of the valve inlet and two coronary arteries at the peak of systole for the first boundary condition; all other outlets had a constant average pressure of 0 Pa. The second boundary condition calculated mass flow rate using half the flow rate at the peak of systole to approximate pulsatile flow conditions when the valve is almost fully open. All other outlets had a constant average pressure of 0 Pa. Table 2 displays flow rates used during peak and half of peak systole at the valve inlet and coronaries.

	Valve Inlet	Right Coronary	Left Coronary
Flow during peak systole	25 L/min	0.015 L/min	0.05 L/min
Flow during half of peak systole	12.5 L/min	0.0075 L/min	0.025 L/min

Table 2: Valve inlet and coronary flow rates used in the computational simulations.

The convergence criterion was 1e-6 for the continuity, X, Y, and Z momentum equations. All other solver conditions were set to default in ANSYS Fluent, with a minimum of 750 iterations being run for each simulation using standard initialization at the inlet. Residuals were monitored, and simulations were stopped once residuals became steady. Using simulation results, the volumetric flow rates and flow percentages through the descending aorta and branches were derived during peak and half of peak systole.

Chapter 3: Results

Velocity vectors for patient 1 during peak systole at the inlet was ~0.75 m/s (Figures 3-1 to 3-8), decreasing as the fluid flowed through the ascending aorta. Vortices were present at some locations of the aortic arch and left and right coronaries. The highest-pressure values were observed at the ascending aorta and the entrances of the greater arteries (5.33 – 6.78 mmHg), while the lowest pressures were located at the descending aorta (0.67 – 0.95 mmHg) (Figure 3-9). Wall shear stress (WSS) values were distributed almost uniformly throughout the model (0.00777 – 22.87 Pa) (Figure 3-10).

Velocity vectors for patient 2 during peak systole flow indicate fluid flow of ~0.95 m/s at the inlet, decreasing as the fluid travels through the ascending aorta. Vortices are present in small quantities at the left and right coronaries and in the ascending aorta. The highest pressure values were observed at the ascending aorta (4.82 – 5.61 mmHg), and the lowest pressure values were seen at the descending aorta (0.138 – 0.919 mmHg). WSS was distributed almost uniformly, with higher values at the inlet and greater arteries (13.1 – 26.2 Pa).

Figure 3-1: Velocity contours observed during peak systole using planes through the right coronary (RC) in both patients.

Figure 3-2: Velocity contours observed during peak systole using planes through the left coronary (LC) in both patients.

Figure 3-3: Velocity contours observed during peak systole using planes through the non-coronary (NC) in both patients.

Figure 3-4: Velocity contours observed during peak systole using planes through the center of the valve in both patients.

Figure 3-5: Velocity contours observed during peak systole using planes through the center of the valve in both patients.

Figure 3-6: Velocity contours observed during peak systole using planes through the center of the valve in both patients.

25

Figure 3-7: Velocity contours observed during peak systole using planes through the center of the valve in both patients.

Figure 3-8: Velocity contours observed during peak systole using planes through the center of the valve in both patients.

26

Figure 3-9: Pressure values for patient 1 (left) and patient 2 (right) during peak systole.

Figure 3-10: Wall shear stress values for patient 1 (left) and patient 2 (right) during peak systole.

Velocity vectors for patient 1 during half of peak systole flow indicate an average fluid velocity of 0.45 m/s at the inlet (Figures 3-11 to 3-18), decreasing as the fluid travels through the ascending aorta. Vortices are observed at the left and right coronaries. Pressure values were highest at the ascending aorta and entry points of the branches (1.52 – 1.91 mmHg) (Figure 3-19). The descending aorta had the lowest pressure values between -0.0541 – 0.339 mmHg. Wall shear stresses were almost normally distributed with values between 0.0031 – 7.455 Pa (Figure 3-20).

Velocity vectors at the inlet for patient 2 during half of peak systole flow were observed to be ~0.53 m/s, decreasing as the fluid flowed through the ascending aorta. Vortices are observed at the left and right coronary arteries. The highest-pressure values for patient 2 during half of peak systole flow were in the ascending aorta (1.33 – 1.69 mmHg), while the lowest values were observed in the descending aorta (-0.106 – 0.432 mmHg). Wall shear stresses were almost uniformly distributed, with higher values appearing at the ascending aorta and aortic arch (0.003938 – 9.062 Pa). Table 3 displays the calculated volumetric flow rates and flow rate percentages for both patients during different flows.
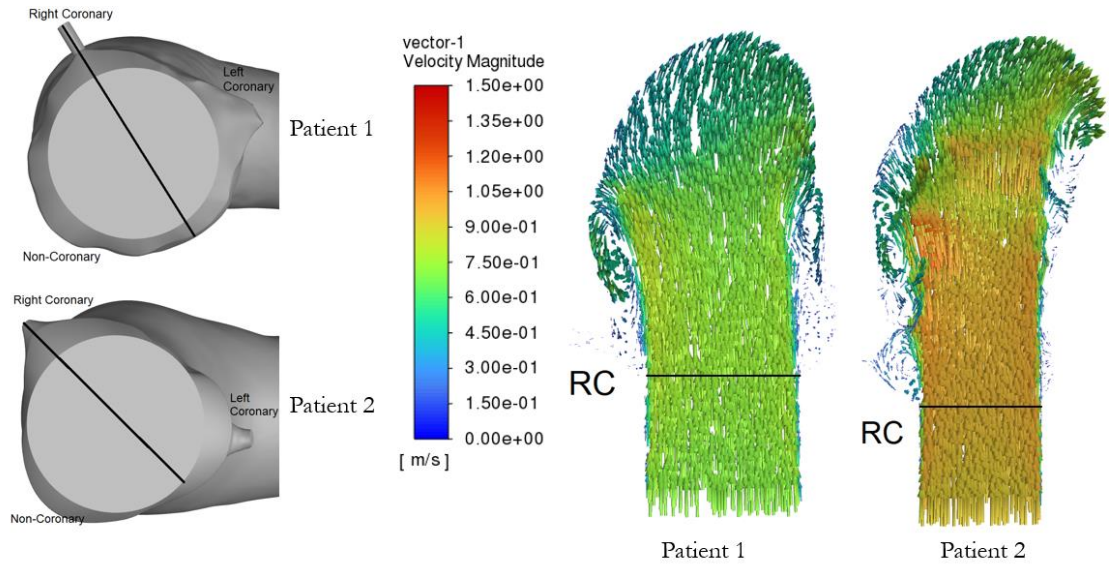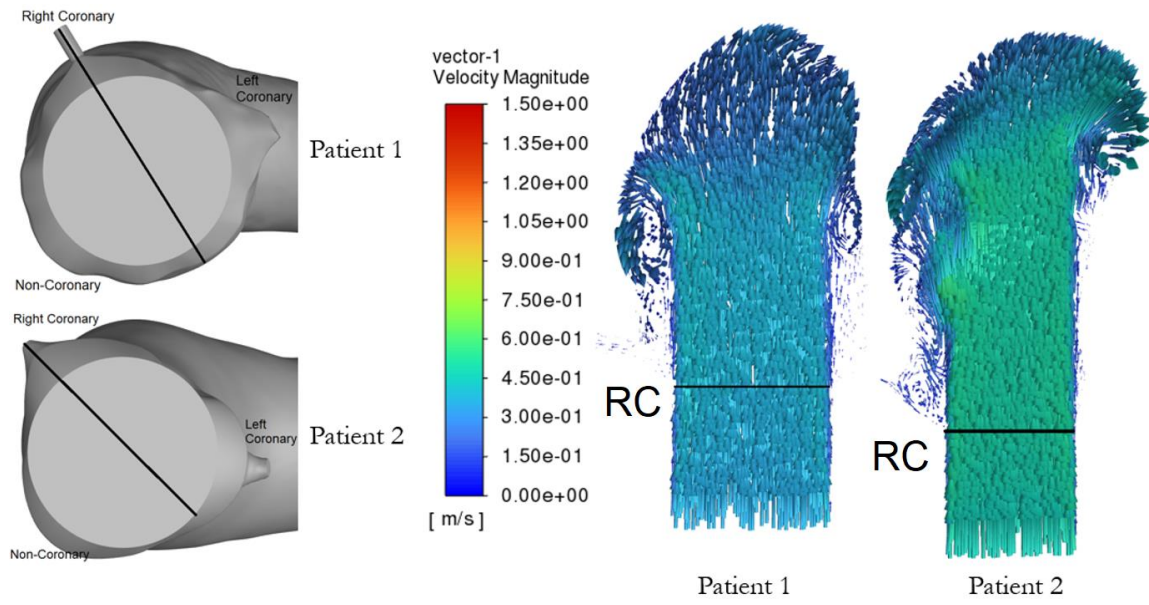
Figure 3-11: Velocity contours observed during half of peak systole using planes through the right coronary in both patients.
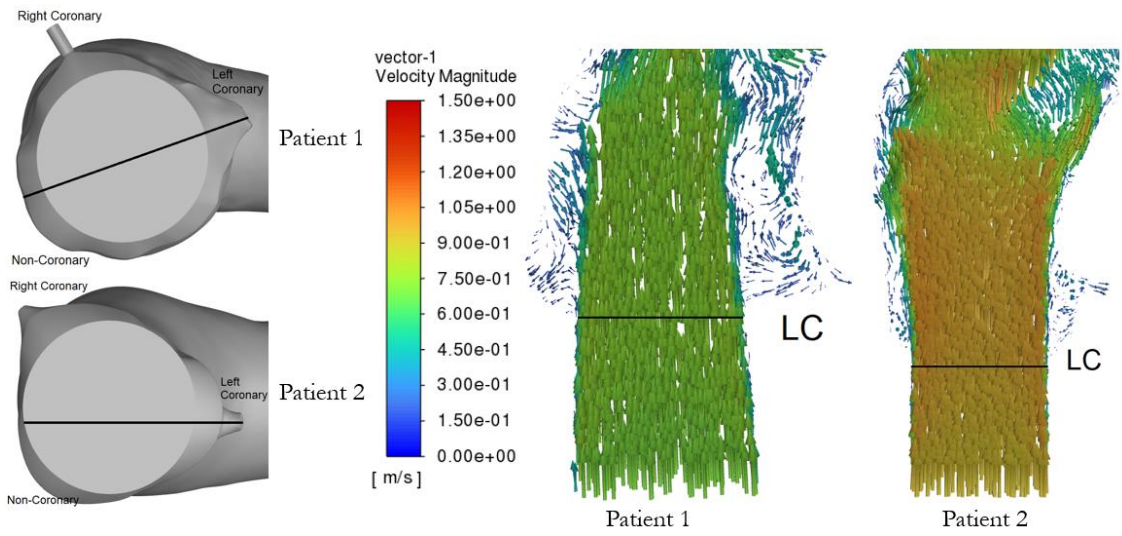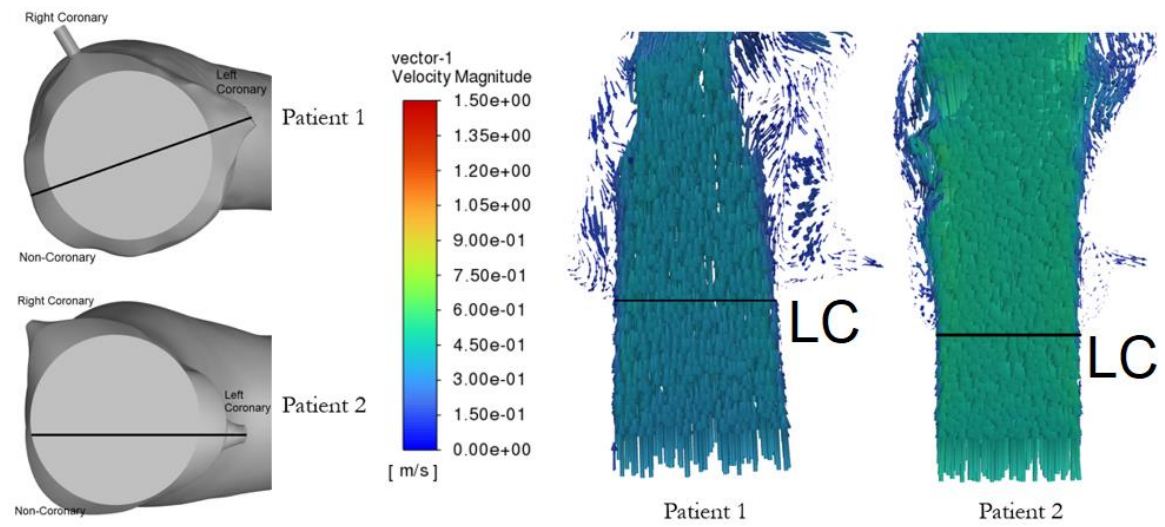

Figure 3-12: Velocity contours observed during half of peak systole using planes through the left coronary in both patients.
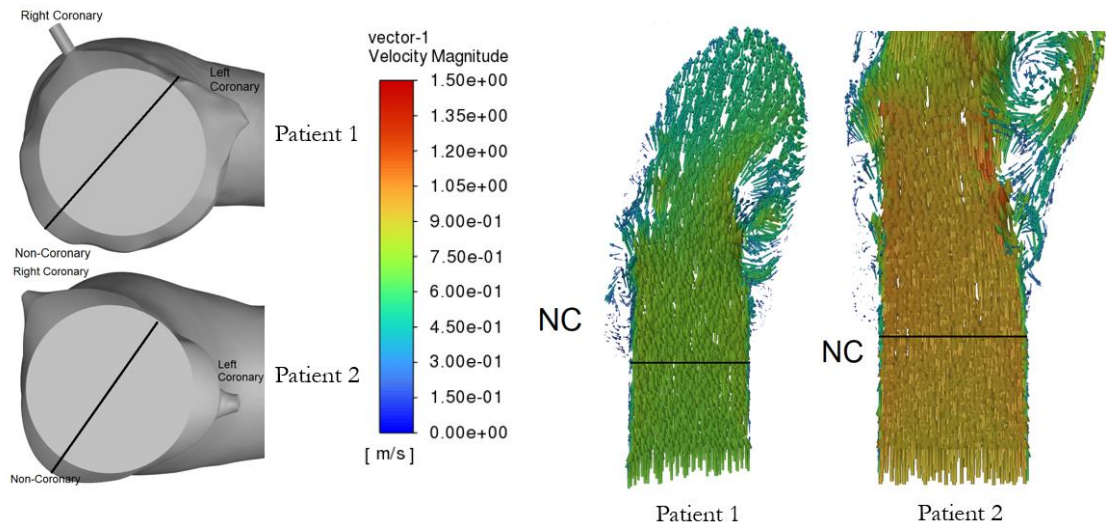
29
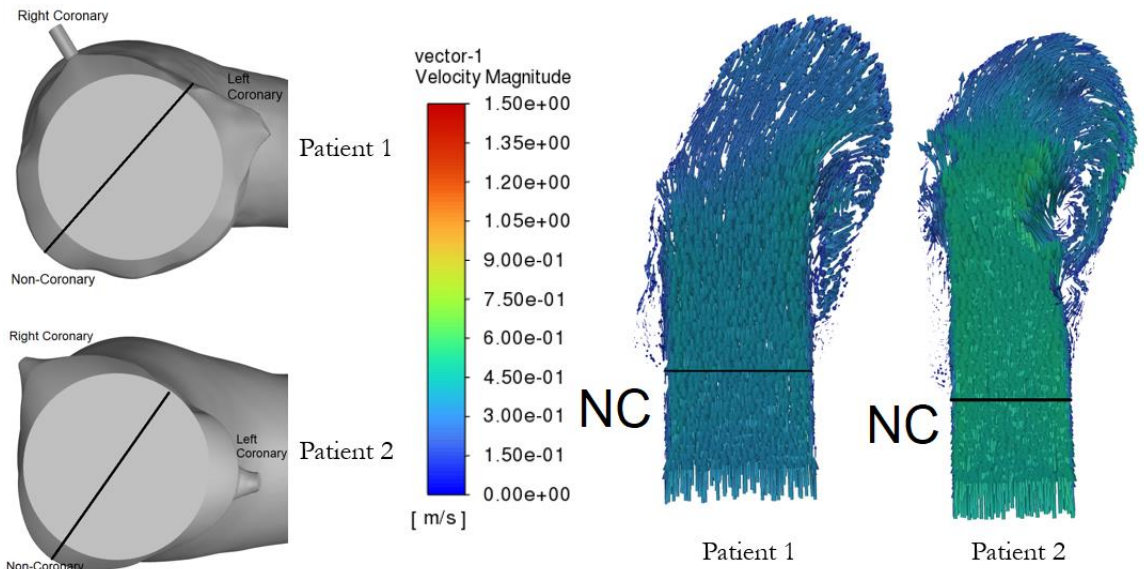
Figure 3-13: Velocity contours observed during half of peak systole using planes through the non-coronary in both patients.
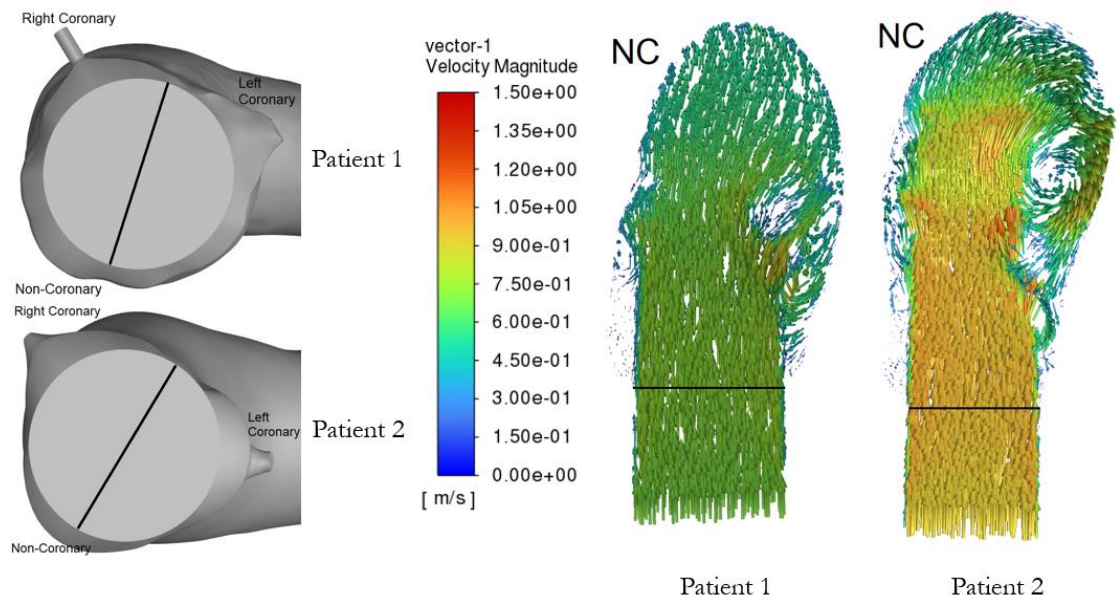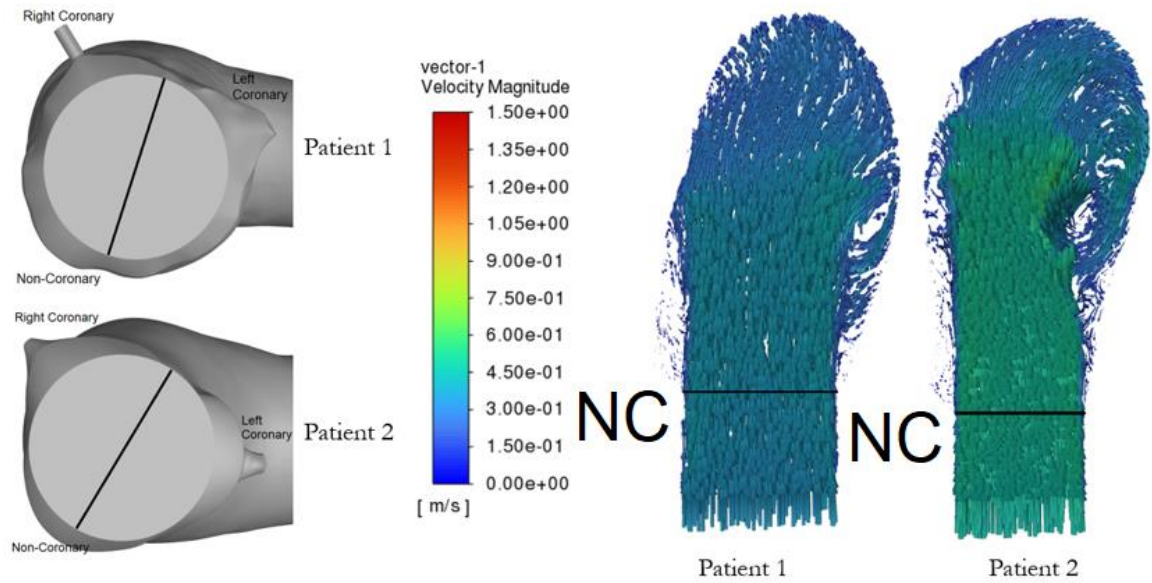

Figure 3-14: Velocity contours observed during half of peak systole using planes through the center of the valve for both patients.
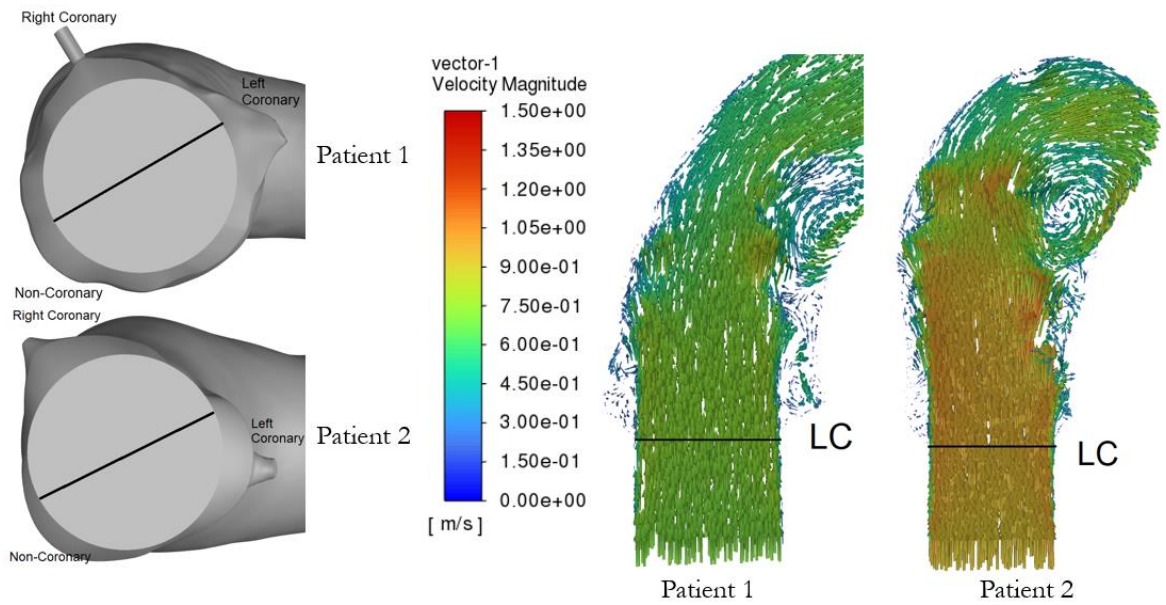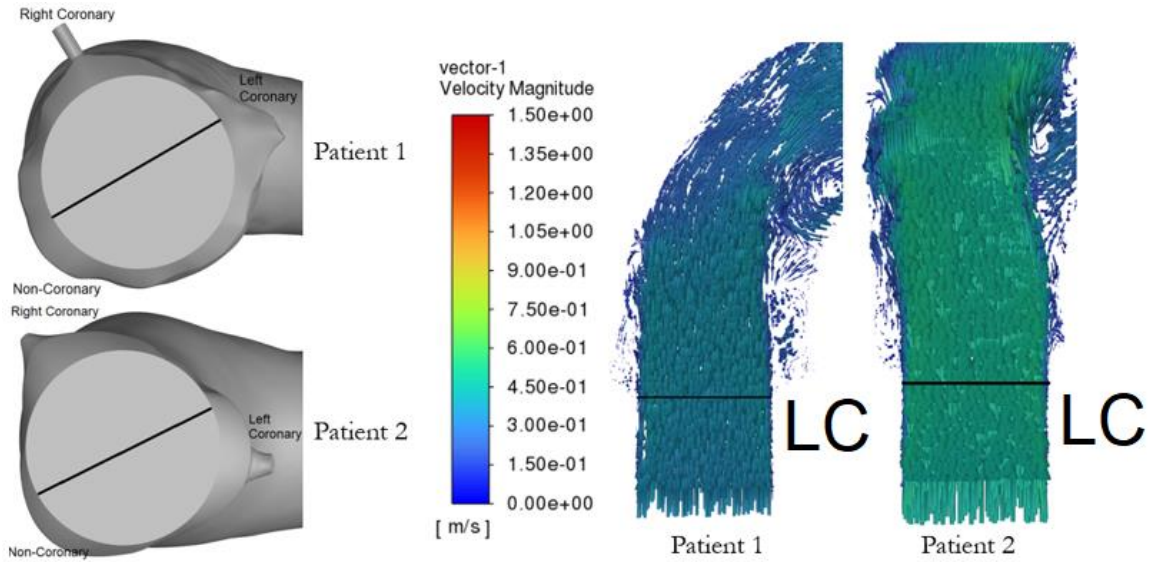
Figure 3-15: Velocity contours observed during half of peak systole using planes through the center of the valve for both patients.
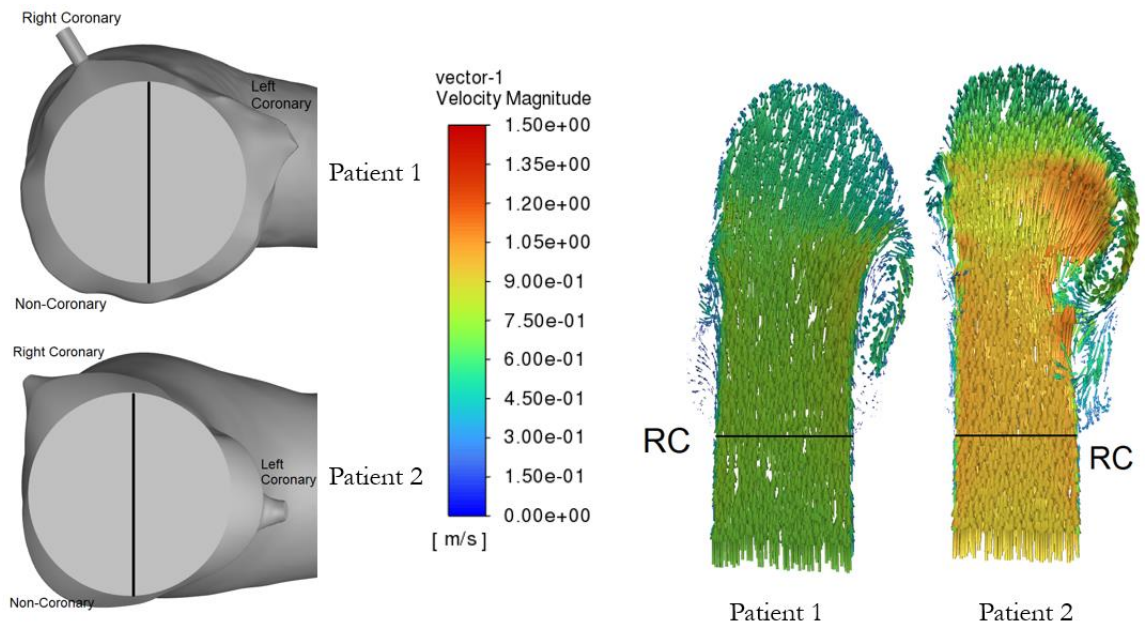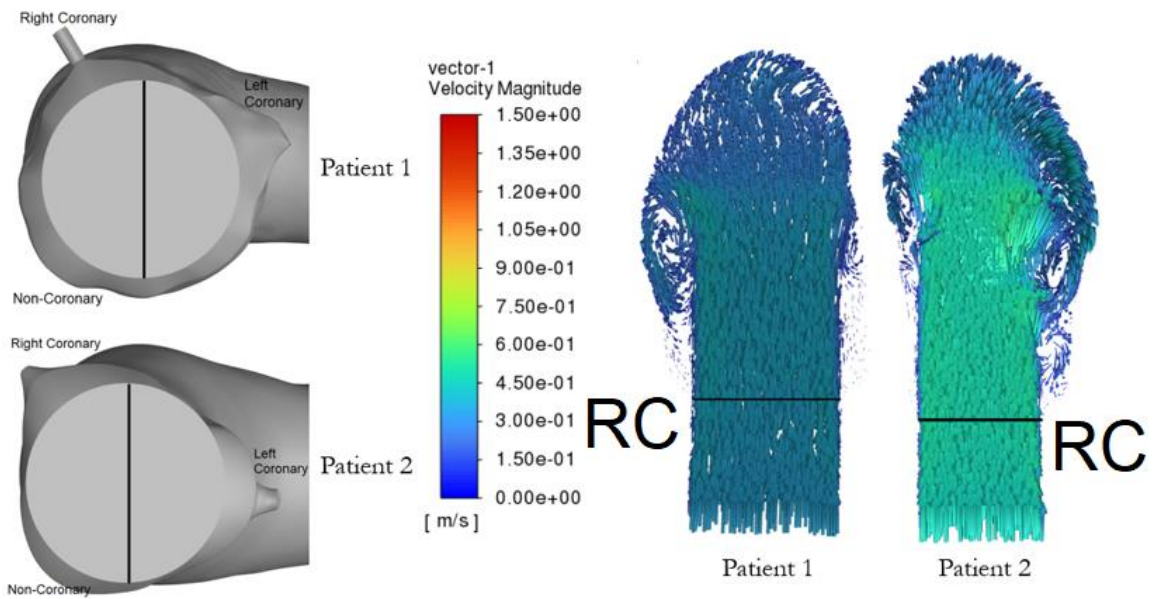

Figure 3-16: Velocity contours observed during half of peak systole using planes through the center of the valve for both patients.
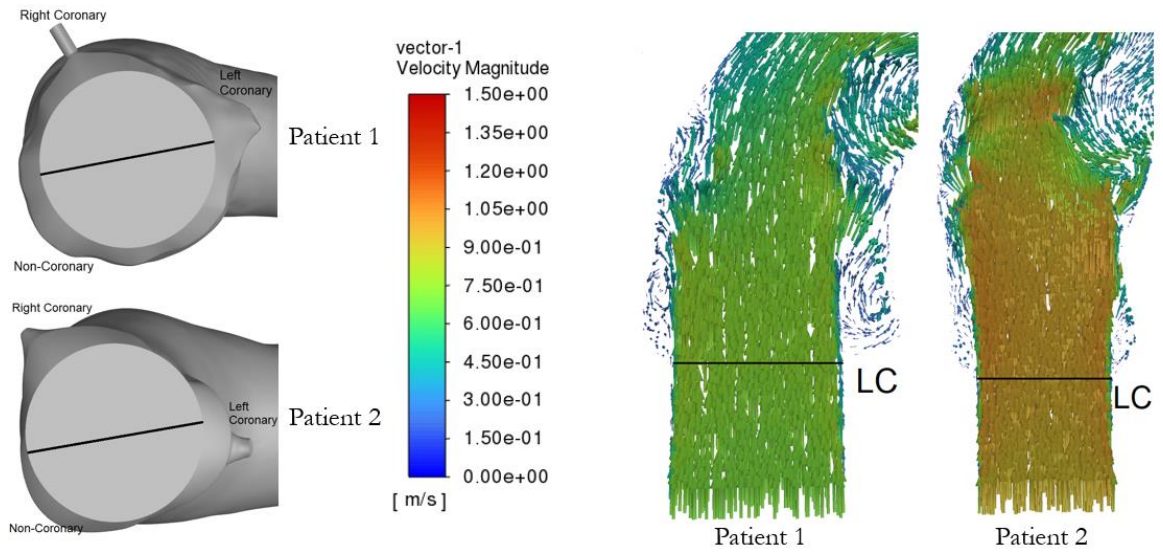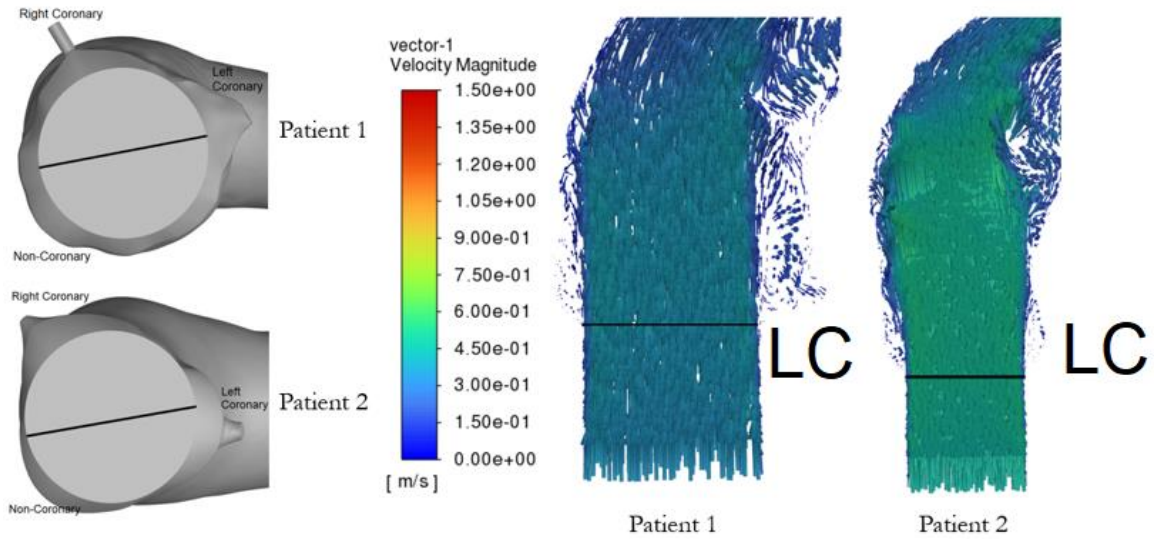
Figure 3-17: Velocity contours observed during half of peak systole using planes through the center of the valve for both patients.
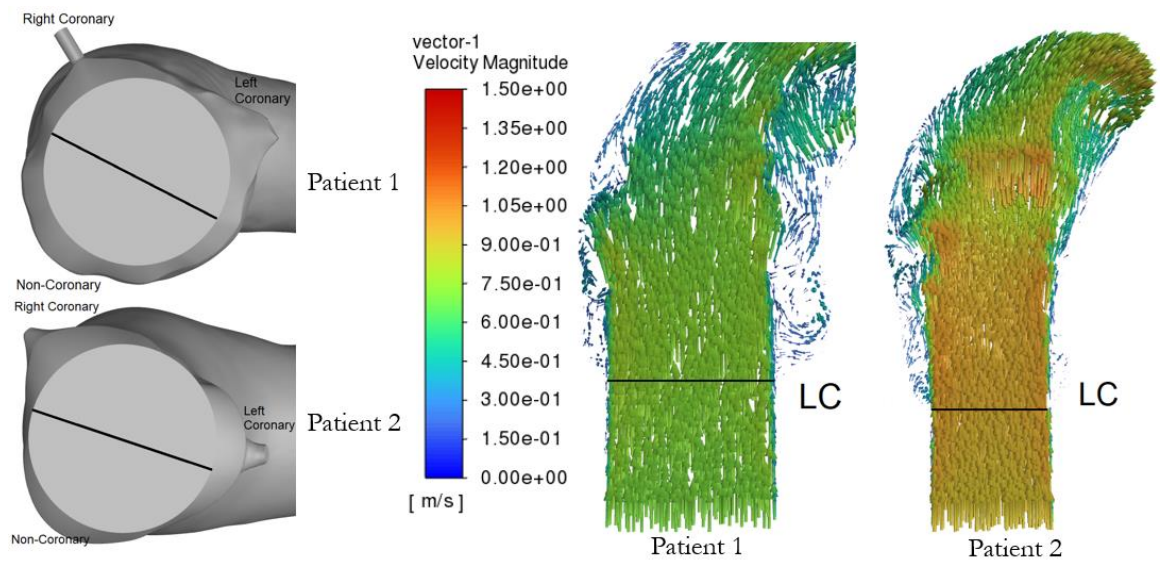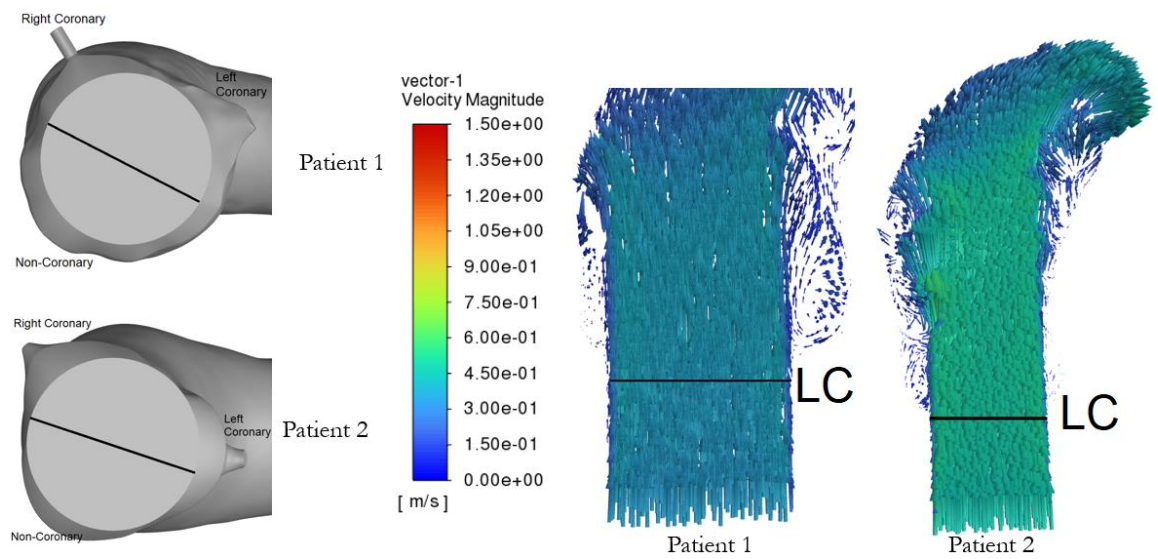

Figure 3-18: Velocity contours observed during half of peak systole using planes through the center of the valve for both patients.
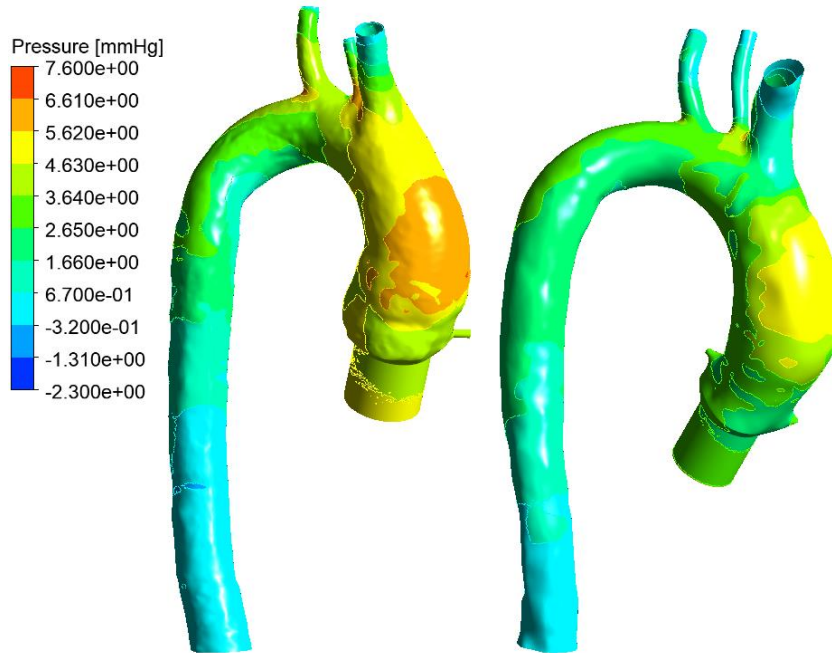
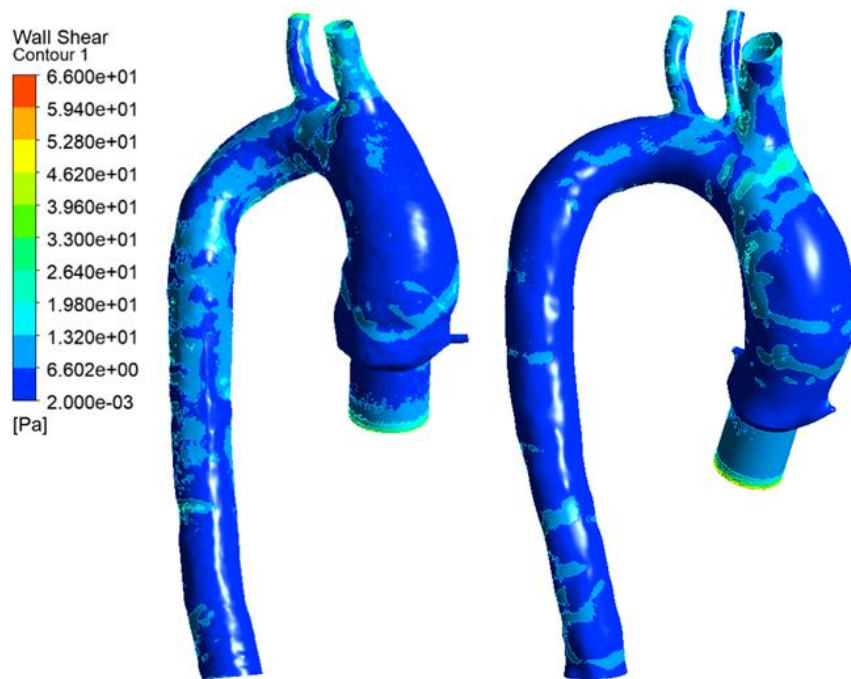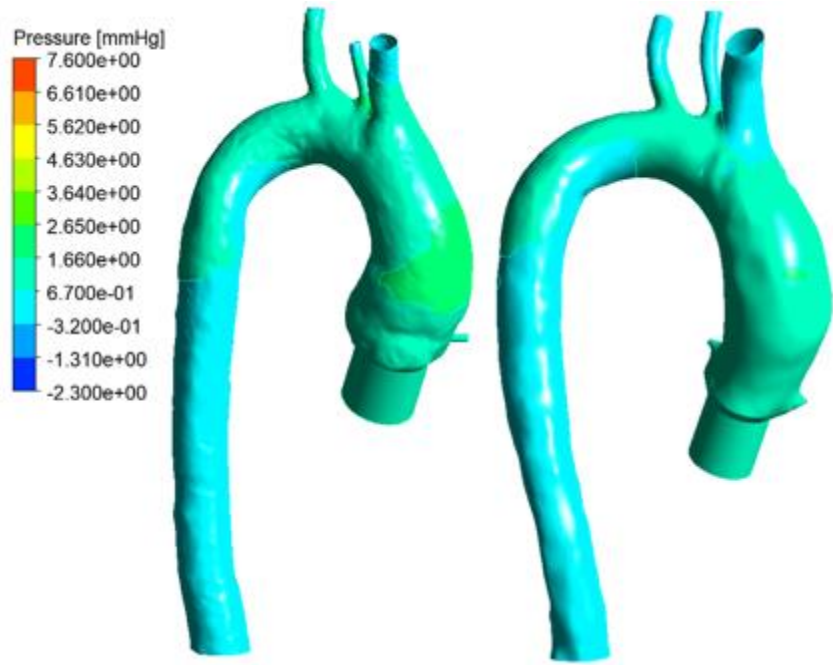Figure 3-19: Pressure values for patient 1 (left) and patient 2 (right) during half of peak systole.
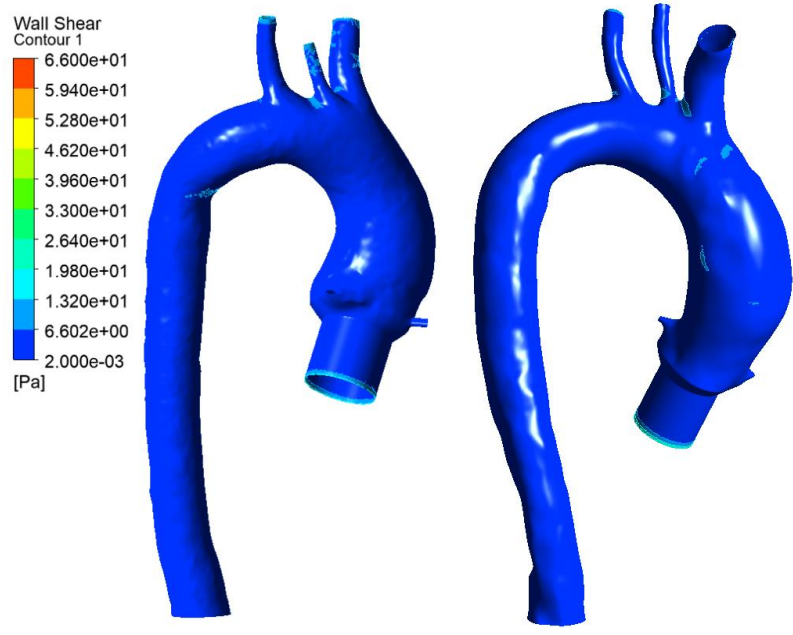
Figure 3-20: Wall shear stress values for patient 1 (left) and patient 2 (right) during half of peak systole.

	Patient	Descending Aorta	Brachiocephalic Artery	Left Common Carotid Artery	Left Subclavian Artery
Flow during peak systole	1	17.11 L/min (~68.4%)	5.195 L/min (~20.8%)	0.8064 L/min (~3.22%)	1.828 L/min (~7.31%)
	2	12.94 L/min (~52%)	8.628 L/min (~34.5%)	1.273 L/min (~5.09%)	2.085 L/min (~8.33%)
Flow during half of peak systole	1	8.526 L/min (~68.2%)	2.638 L/min (~21.1%)	0.3913 L/min (~3.13%)	0.9084 L/min (~7.27%)
	2	6.696 L/min (~53.6%)	4.233 L/min (~33.8%)	0.5704 L/min (~4.6%)	0.9672 L/min (~7.8%)

Table 3: Volumetric flow rates and percentages for patient 1 and patient 2 at the descending aorta and branches.

Chapter 4: Discussion

Importance of Aortic Root Enlargement

ARE is seen as an important supplement to SAVR in patients with small aortic annuli to mitigate PPM and facilitate ViV TAVR [53, 54]. PPM has been correlated with increased all-cause and cardiac-related mortality after SAVR, early structural valve degeneration, and a higher occurrence of heart failure-related readmission [55, 56]. Recent findings indicate 50% of patients develop moderate or severe PPM after SAVR, indicating a necessity for ARE [57]. Shih et al. [58] reported no differences in 30-day mortality, 5-year survival, or postoperative complications in propensity-matched groups compared to isolated SAVR + ARE and SAVR. Patients undergoing ARE for AVR are more likely to be female and have a smaller indexed EOA [59]. Since these patients have a smaller aortic annulus and a reduced EOA, the absence of ARE may cause a further decrease in EOA after AVR, increasing PPM risks and worse hemodynamic outcomes. Stentless aortic root replacements can be used to avoid PPM, but the procedure may be difficult for surgeons who do not perform ARE procedures frequently [60]. With the advent of TAVR, failing prosthetic aortic valves are often replaced with the ViV approach, and patients undergoing ViV have a high PPM in cases of small bioprosthetic valves [36, 61, 62]. The ViV technique reduces the EOA. Therefore, ARE may benefit

patients undergoing a ViV TAVR by allowing the deployment of larger prosthetics without risk of mortality or adverse events [59].

History of Aortic Root Enlargement

ARE was first developed in the 1970s but has yet to be adopted widely and is performed in less than 10% of SAVRs [63]. Root enlargement techniques include but are not limited to Nicks [40], Manouguian and Seybold-Epting [41], Konno and colleagues [64], and the Yang procedure [49]. The Konno procedure is an anterior annular patch augmentation extending onto the right ventricle but is rarely utilized in adults.

Yang and colleagues have modified their previously reported rectangular/Y-incision patch, which described a "roof technique" to enlarge the sinotubular junction and proximal ascending aorta via a triangular patch superior to the rectangular patch, facilitating closure of the aortotomy [49, 52, 65]. The Yang procedure is superior to previous root enlargement procedures as it facilitates the implantation of valve sizes 2-5 sizes larger than the native annulus, reducing PPM risks and facilitating future ViV TAVR by combining the Y-incision and roof techniques.

Transcatheter Heart Valve Dysfunction

Valvular disease is common in elderly patients. TAVR and SAVR are techniques used to replace the aortic valve in patients with valvular diseases. Bioprosthetic valves are used to avoid anticoagulation risks, but recent studies have indicated associated thrombosis [48, 66] in TAVR and SAVR procedures. Reduced leaflet motion, mean thickness, and one, two, or three affected leaflets are contributing factors affecting

thrombosis occurrence [48] and an indication of transcatheter heart valve (THV) dysfunction. Diagnosis criteria of THV dysfunction are (1) non-recorded moderate or more prosthetic valve regurgitation post-procedure, and (2) an aortic valve area less than 1.2 cm^2 or a mean aortic valve pressure gradient of less than or equal to 20 mmHg or a peak velocity greater than or equal to 3 m/s [67]. THV thrombosis diagnosis can be defined as (1) THV dysfunction after thrombosis occurrence based on new heart failure symptoms after imaging, histopathology findings, or anticoagulation therapy, or (2) detection of mobile mass on a THV suspected of thrombosis in the absence of infection, regardless of THV dysfunction. The commonness of single leaflet thrombosis (SLT) in transcatheter valves is reportedly 13%, while surgical valves have a rate of 4% [48]. Hansson et al. reported THV thrombosis occurred in 7% of patients, with most having SLT [68].

The SAVORY (Subclinical Aortic Valve Bioprosthesis Thrombosis Assessed with Four-Dimensional Computed Tomography) and RESOLVE (Assessment of Transcatheter and Surgical Aortic Bioprosthetic Valve Thrombosis and Its Treatment with Anticoagulation) registries have indicated the THV mechanism (i.e., mechanically-, balloon-expandable) is not the contributing factor to thrombosis. Rather, the intra-annular and supra-annular designs, with supra-annular designs having a higher rate of leaflet thrombosis [48]. Furthermore, an increased rate of THV thrombosis is associated with larger THVs [48, 69].

Increased incidences of thrombus formation on bioprosthetic valves have been associated with comorbidities in patients [70, 71]. These factors include a high body mass

index, low cardiac function, and atrial dilatation and fibrillation. Other contributing factors include root morphology, small valve sizes, and a change or lack of anticoagulation. Anticoagulation will reduce thrombosis and restore leaflet motion after three months, improving hemodynamics in patients. In the absence of anticoagulation, reduced leaflet motion will progress or persist in patients [48, 66].

Flow Stasis

TAVR is a well-established treatment method for patients with severe symptomatic aortic stenosis at high risk for SAVR or inoperable. Valve thrombosis is a significant risk factor associated with AVR. Valve thrombosis leading to reduced leaflet motion has been observed increasingly in TAVR patients and patients undergoing ViV procedures [69, 72-75]. Although the incidence of valve thrombosis in patients undergoing SAVR is considered low (0.03 – 1.46%) [70, 76], leaflet immobility occurrence has been seen to be 13% post-SAVR [75]. After TAVR, thrombus development may occur up to 40% of the time [74]. Thrombotic materials are primarily identified on the aortic side of the leaflets after ViV and TAVR procedures, and valvular thrombosis mainly occurs in the intraanular positioning of TAV devices after TAVR. Valve thrombosis may lead to a higher prevalence of transient ischemic attacks (TIA) and strokes [75].

Vahidkhah et al. [77] determined greater blood stasis on transcatheter aortic valve leaflets near the valve frame may be induced by the geometric restriction of transcatheter aortic valve leaflets and their intraanular location. They observed high blood residence

38

time on all three leaflets of a TAV model. Clinical studies on TAV noncoronary versus coronary leaflet thrombosis and blood residence time results are consistent. These studies also reported valvular thrombosis formation on all leaflets post-TAVR and ViV [74, 75].

Leaflet Thrombosis

In 15-30% of individuals receiving a bioprosthetic valve for aortic stenosis, subclinical leaflet thrombosis with or without impaired leaflet motion has been noted [48, 75, 78]. Isolated leaflet thrombosis is also known as hypoattenuated leaflet thrombosis (HALT) on multidetector computed tomography. Reduced leaflet mobility (RELM) can be associated with HALT and is known as hypo-attenuation affecting motion (HAM). Bogyi et al. [79] analyzed SLT after AVR. They discovered 18.6% (207/1112) of patients undergoing TAVR developed SLT while 19% (91/479) of patients developed SLT undergoing SAVR. 7.2% (433/5974) of patients with intraanular valves developed SLT compared to 1.6% (61/3720) of patients with supraanular valves, indicating risk factors associated with intraanular positioning. Risks of TIA and stroke were compared to patients with and without SLT. 6% (22/368) of patients with SLT developed TIA or stroke during follow-up compared to 4.7% (152/3253) patients without SLT. This indicates TIA or stroke is 2.6-fold higher when diagnosed with SLT. ViV TAVR is also a positive predictor for SLT.

Sondergaard et al. [78] analyzed SLT affecting motion in bioprosthetic heart valves. They identified HALT was observed in 38.1% (32) of patients, while HAM was observed in 50% of HALT cases. The occurrence was similar in SAVR and TAVR.

Preliminary Conclusions

Computational simulations demonstrated similarities and differences in blood flow characteristics between patient 1 and patient 2 after root enlargement using the Yang procedure. Both patients displayed similar velocity patterns at the aortic root, ascending aorta, and left and right coronaries. Rotational patterns were observed at the coronaries, ascending aorta, and aortic arch. The secondary flow at the aortic arch was caused by the flow direction respective to the valve intersecting with the native curved geometry of the aorta. Patient 1 had a greater percentage of blood flow through the descending aorta compared to patient 2 during peak systole. However, the fluid magnitude of patient 1 was ~21% less than patient 2. Furthermore, flow at the coronaries was observed to be slower in patient 1. A greater fluid velocity at the inlet caused increased circulation at the coronaries for patient 2. A slower flow, as seen in patient 1, may result in conditions such as flow stasis and thrombosis. Additionally, introducing a foreign bioprosthetic valve in patients concurrently poses a risk of thrombosis [80]. Therefore, cardiovascular risks may be elevated in patients who have undergone ARE using the Yang procedure.

Pressure around the aortic root and ascending aorta was higher for patient 1 during peak systole, reaching the maximum value at the ascending aorta for both patients. Peak pressure for patient 1 at the ascending aorta was ~17.4% higher than patient 2. WSS remained similar between both patients for both flows at the aortic root and ascending aorta. However, peak WSS for patient 1 was ~12.2% lower than patient 2. Low WSS indicates a possibility of flow stasis due to low velocity.

Taken together, the data of the simulations indicate the results are applicable in planning future surgical procedures in patients. A study by Hellmeier et al. investigated MRI-based CFD simulations in patients pre-surgery to examine the hemodynamic outcomes of different valve prostheses [81]. Another study by Nauta et al. modeled three virtual aortic interventions to assess their effect on thrombosis [82]. They discovered single-branched endografting, conformable endografting, and open surgical repair offered different hemodynamic outcomes. They concluded CFD may assist in predicting thrombotic events and help with surgical repair strategies in patients. These studies suggest CFD simulations may assist in the optimization of surgical decisions pre-surgery in patients.

Limitations of the Study

A total of six patient data were available, but only two patients were compared due to the time limitations of the study. Future studies should incorporate data from all patients to further understand hemodynamics regarding the Yang procedure. Simplified valve and aorta geometries were created to replicate the function of the Carpentier-Edwards PERIMOUNT Magna Ease valve. Further research should utilize the original valve geometry. This study incorporated steady, laminar flow and did not consider pulsatile flow or RCR boundary conditions at the outlets. Although pulsatile flow was mimicked using steady, laminar flow during half of peak systole, future simulations should consider simulating pulsatile flow and RCR conditions. Patient follow-up data was not available at the time of the study. Long-term patient follow-ups must be

investigated to understand the effects of the Yang procedure. Finally, the simulation

results must be validated. Patient follow-ups, echocardiography, and in-vitro

experimental setups are suitable to assess the validity of this study.

Chapter 5: Conclusions

The Yang procedure is an effective technique used to enlarge the aortic root in patients with small annuli. Computational simulations highlighted differences in blood flow characteristics in the aortic root and valve regions after aortic root enlargement compared to the control subject. Surgeons can employ simulation results to plan surgical procedures in patients. The long-term effects of the Yang procedure on patient hemodynamics, the aorta, and bioprosthetic valves must be studied as slower flow through the coronary arteries and ascending aorta may result in flow stasis and thrombosis.

References

1. Mahadevan, V., *Anatomy of the heart.* Surgery (Oxford), 2018. **36**(2): p. 43-47.
2. Bianco, C., *How your heart works.* HowStuffWorks. Archived from the original on 29 July 2016. Retrieved 14 August 2016, 2004.
3. Sacks, M.S., W.D. Merryman, and D.E. Schmidt, *On the biomechanics of heart valve function.* Journal of biomechanics, 2009. **42**(12): p. 1804-1824.
4. Yoganathan, A.P., Z. He, and S. Casey Jones, *Fluid mechanics of heart valves.* Annu. Rev. Biomed. Eng., 2004. **6**: p. 331-362.
5. Gopalan, C. and E. Kirk, *Biology of Cardiovascular and Metabolic Diseases*. 2022: Academic Press.
6. Carabello, B.A., *Introduction to aortic stenosis.* Circulation research, 2013. **113**(2): p. 179-185.
7. CARABELLO, B.A., *AORTIC STENOSIS.* N Engl J Med, 2002. **346**(9).
8. Vaidya, Y.P., S.M. Cavanaugh, and A.A. Sandhu, *Surgical aortic valve replacement in small aortic annulus.* Journal of Cardiac Surgery, 2021. **36**(7): p. 2502-2509.

9. Nishimura, R.A., et al., *2014 AHA/ACC guideline for the management of patients with valvular heart disease: a report of the American College of Cardiology/American Heart Association Task Force on Practice Guidelines.* Circulation, 2014. **129**(23): p. e521-e643.
10. Bahlmann, E., et al., *Small aortic root in aortic valve stenosis: clinical characteristics and prognostic implications.* European Heart Journal–Cardiovascular Imaging, 2017. **18**(4): p. 404-412.
11. Freitas-Ferraz, A.B., et al., *Aortic Stenosis and Small Aortic Annulus: Clinical Challenges and Current Therapeutic Alternatives.* Circulation, 2019. **139**(23): p. 2685-2702.
12. Gopal, S., J.M. Hauser, and S.K. Mahboobi, *Mechanical Aortic Valve Replacement.* 2020.
13. Kostyunin, A.E., et al., *Degeneration of bioprosthetic heart valves: update 2020.* Journal of the American Heart Association, 2020. **9**(19): p. e018506.
14. Khan, M.G., *Valve Diseases*, in *Encyclopedia of Heart Diseases*, M.G. Khan, Editor. 2006, Academic Press: Burlington. p. 599-606.
15. Schoen, F.J. and J. Butany, *Chapter 13 - Cardiac Valve Replacement and Related Interventions*, in *Cardiovascular Pathology (Fourth Edition)*, L.M. Buja and J. Butany, Editors. 2016, Academic Press: San Diego. p. 529-576.
16. Ramlawi, B., M. Ramchandani, and M.J. Reardon, *Surgical approaches to aortic valve replacement and repair—insights and challenges.* Interventional Cardiology Review, 2014. **9**(1): p. 32.
17. Rao, V., et al., *A novel comparison of stentless versus stented valves in the small aortic root.* The Journal of Thoracic and Cardiovascular Surgery, 1999. **117**(3): p. 431-438.

18.   Gulbins, H. and H. Reichenspurner, *Which patients benefit from stentless aortic valve replacement?* The Annals of thoracic surgery, 2009. **88**(6): p. 2061-2068.

19.   Kobayashi, J., *Stentless aortic valve replacement: an update.* Vascular health and risk management, 2011: p. 345-351.

20.   Kunihara, T., et al., *Root replacement using stentless valves in the small aortic root: a propensity score analysis.* The Annals of thoracic surgery, 2006. **82**(4): p. 1379-1384.

21.   Dasi, L.P., et al., *On the mechanics of transcatheter aortic valve replacement.* Annals of biomedical engineering, 2017. **45**: p. 310-331.

22.   Lederman, R.J., et al., *Transcaval Versus Transaxillary TAVR in Contemporary Practice: A Propensity-Weighted Analysis.* JACC: Cardiovascular Interventions, 2022. **15**(9): p. 965-975.

23.   Faroux, L., et al., *Coronary Artery Disease and Transcatheter Aortic Valve Replacement: JACC State-of-the-Art Review.* Journal of the American College of Cardiology, 2019. **74**(3): p. 362-372.

24.   Sellke, F. and M. Ruel, *Atlas of Cardiac Surgical Techniques: A Volume in the Surgical Techniques Atlas Series*. 2009: Elsevier Health Sciences.

25.   León del Pino, M.d.C., et al., *Prosthesis-patient mismatch after transcatheter aortic valve replacement: prevalence and medium term prognostic impact.* The international journal of cardiovascular imaging, 2019. **35**: p. 827-836.

26.   Kalavrouziotis, D., et al., *Transcatheter aortic valve implantation in patients with severe aortic stenosis and small aortic annulus.* Journal of the American College of Cardiology, 2011. **58**(10): p. 1016-1024.

27.   Tasca, G., et al., *Early hemodynamic evaluation of Trifecta and Freestyle bioprostheses in patients with a small aortic root: preliminary results from a prospective randomized study.* The Journal of Heart Valve Disease, 2014. **23**(5): p. 633-641.

28.   Wollersheim, L.W., et al. *Stentless vs stented aortic valve bioprostheses in the small aortic root*. in *Seminars in Thoracic and Cardiovascular Surgery*. 2016. Elsevier.

29.   Guimarães, L., et al., *Valve hemodynamics following transcatheter or surgical aortic valve replacement in patients with small aortic annulus.* The American journal of cardiology, 2020. **125**(6): p. 956-963.

30.   Kamioka, N., et al., *Valve hemodynamics and clinical outcomes after transcatheter aortic valve replacement for a small aortic annulus.* International heart journal, 2019. **60**(1): p. 86-92.

31.   Olivier Dionne, P., et al., *Early hemodynamic results in patients with small aortic annulus after aortic valve replacement.* Innovations, 2017. **12**(4): p. 254-258.

32.   Vemulapalli, S., et al., *Procedural volume and outcomes for transcatheter aortic-valve replacement.* New England Journal of Medicine, 2019. **380**(26): p. 2541-2550.

33.   Salaun, E., et al., *Bioprosthetic aortic valve durability in the era of transcatheter aortic valve implantation.* Heart, 2018. **104**(16): p. 1323-1332.

34.   Milburn, K., V. Bapat, and M. Thomas, *Valve-in-valve implantations: is this the new standard for degenerated bioprostheses? Review of the literature.* Clinical Research in Cardiology, 2014. **103**: p. 417-429.

35.   Khan, J.M., et al., *Transcatheter Laceration of Aortic Leaflets to Prevent Coronary Obstruction During Transcatheter Aortic Valve Replacement: Concept to First-in-Human.* JACC: Cardiovascular Interventions, 2018. **11**(7): p. 677-689.

36.   Dvir, D., et al., *Transcatheter aortic valve replacement for degenerative bioprosthetic surgical valves: results from the global valve-in-valve registry.* Circulation, 2012. **126**(19): p. 2335-2344.

37.   Saxon, J.T., et al., *Complications of bioprosthetic valve fracture as an adjunct to valve-in-valve TAVR.* Structural Heart, 2019. **3**(2): p. 92-99.

38.   Zenses, A.-S., et al., *Haemodynamic outcomes following aortic valve-in-valve procedure.* Open heart, 2018. **5**(2): p. e000854.

39.   Massias, S.A., et al., *Aortic root enlargement: when and how.* Journal of Cardiac Surgery, 2021. **36**(1): p. 229-235.

40.   Nicks, R., T. Cartmill, and L. Bernstein, *Hypoplasia of the aortic root: the problem of aortic valve replacement.* Thorax, 1970. **25**(3): p. 339-346.

41.   Manouguian, S. and W. Seybold-Epting, *Patch enlargement of the aortic valve ring by extending the aortic incision into the anterior mitral leaflet: new operative technique.* The Journal of thoracic and cardiovascular surgery, 1979. **78**(3): p. 402-412.

42.   Sá, M.P.B.O., et al., *Impact of surgical aortic root enlargement on the outcomes of aortic valve replacement: a meta-analysis of 13 174 patients.* Interactive CardioVascular and Thoracic Surgery, 2019. **29**(1): p. 74-82.

43.   Yu, W., et al., *Aortic root enlargement is safe and reduces the incidence of patient-prosthesis mismatch: a meta-analysis of early and late outcomes.* Canadian Journal of Cardiology, 2019. **35**(6): p. 782-790.

44.   Haunschild, J., et al., *Aortic root enlargement to mitigate patient–prosthesis mismatch: do early adverse events justify reluctance?* European Journal of Cardio-Thoracic Surgery, 2019. **56**(2): p. 335-342.

45.   Bishop, M.A. and K. Borsody, *Manougian.* 2020.

46.   Nyamande, D. and P.S. Ramoroko, *The Yang procedure: Renaming the recently described "Y" incision/rectangular patch aortic annulus enlargement technique.* JTCVS Techniques, 2023. **18**: p. 43.

47.   Dhareshwar, J., et al., *Aortic root enlargement: What are the operative risks?* The Journal of Thoracic and Cardiovascular Surgery, 2007. **134**(4): p. 916-924.

48.   Chakravarty, T., et al., *Subclinical leaflet thrombosis in surgical and transcatheter bioprosthetic aortic valves: an observational study.* The Lancet, 2017. **389**(10087): p. 2383-2392.

49.   Yang, B., *A novel simple technique to enlarge the aortic annulus by two valve sizes.* JTCVS techniques, 2021. **5**: p. 13-16.

50.   Yang, B., C. Ghita, and S. Palmer, *Y-incision aortic root enlargement with modified aortotomy upsizing the annulus by 5 valve sizes.* The Annals of Thoracic Surgery, 2022. **114**(6): p. e479-e481.

51. Yang, B., et al., *Early outcomes of the Y-incision technique to enlarge the aortic annulus 3 to 4 valve sizes.* The Journal of Thoracic and Cardiovascular Surgery, 2022.

52. Yang, B., A. Naeem, and S. Palmer, *"Roof" technique—a modified aortotomy closure in Y-incision aortic root enlargement upsizing 3-4 valve sizes.* JTCVS techniques, 2022. **12**: p. 33-36.

53. Bianco, V., et al., *Long-term hospital readmissions after surgical vs transcatheter aortic valve replacement.* The Annals of Thoracic Surgery, 2019. **108**(4): p. 1146-1152.

54. Sultan, I., et al., *Management of coronary obstruction following transcatheter aortic valve replacement.* Journal of cardiac surgery, 2017. **32**(12): p. 777-781.

55. Flameng, W., et al., *Prosthesis-patient mismatch predicts structural valve degeneration in bioprosthetic heart valves.* Circulation, 2010. **121**(19): p. 2123-2129.

56. Head, S.J., et al., *The impact of prosthesis–patient mismatch on long-term survival after aortic valve replacement: a systematic review and meta-analysis of 34 observational studies comprising 27 186 patients with 133 141 patient-years.* European heart journal, 2012. **33**(12): p. 1518-1529.

57. Fallon, J.M., et al., *The incidence and consequence of prosthesis-patient mismatch after surgical aortic valve replacement.* The Annals of thoracic surgery, 2018. **106**(1): p. 14-22.

58. Shih, E., et al., *Outcomes of aortic root enlargement during isolated aortic valve replacement.* Journal of Cardiac Surgery, 2022. **37**(8): p. 2389-2394.

59. Rocha, R.V., et al., *Surgical enlargement of the aortic root does not increase the operative risk of aortic valve replacement.* Circulation, 2018. **137**(15): p. 1585-1594.

60. Yousef, S. and I. Sultan, *Aortic root enlargement: Just do it.* Journal of Cardiac Surgery, 2022. **37**(8): p. 2395-2396.

61. Dvir, D., et al., *Transcatheter aortic valve implantation in failed bioprosthetic surgical valves.* Jama, 2014. **312**(2): p. 162-170.

62. Webb, J.G., et al., *Transcatheter aortic valve implantation within degenerated aortic surgical bioprostheses: PARTNER 2 valve-in-valve registry.* Journal of the American College of Cardiology, 2017. **69**(18): p. 2253-2262.

63. Tam, D.Y., et al., *Surgical valve selection in the era of transcatheter aortic valve replacement in the Society of Thoracic Surgeons Database.* The Journal of Thoracic and Cardiovascular Surgery, 2020. **159**(2): p. 416-427. e8.

64. Konno, S., et al., *A new method for prosthetic valve replacement in congenital aortic stenosis associated with hypoplasia of the aortic valve ring.* The Journal of thoracic and cardiovascular surgery, 1975. **70**(5): p. 909-917.

65. Yang, B. and A. Naeem, *AY incision and rectangular patch to enlarge the aortic annulus by three valve sizes.* The Annals of thoracic surgery, 2021. **112**(2): p. e139-e141.

66. Bax, J.J. and G.W. Stone, *Bioprosthetic surgical and transcatheter heart valve thrombosis.* The Lancet, 2017. **389**(10087): p. 2352-2354.

67. Kanjanauthai, S., et al., *Subclinical leaflet thrombosis following transcatheter aortic valve replacement.* Journal of interventional cardiology, 2018. **31**(5): p. 640-647.

68. Franzone, A., et al., *Transcatheter aortic valve thrombosis: incidence, clinical presentation and long-term outcomes.* European heart journal-cardiovascular imaging, 2018. **19**(4): p. 398-404.

69. Latib, A., et al., *Treatment and clinical outcomes of transcatheter heart valve thrombosis.* Circulation: Cardiovascular Interventions, 2015. **8**(4): p. e001779.

70. Egbe, A.C., et al., *Bioprosthetic valve thrombosis versus structural failure: clinical and echocardiographic predictors.* Journal of the American College of Cardiology, 2015. **66**(21): p. 2285-2294.

71. Mack, M. and D. Holmes, *Bioprosthetic valve thrombosis: The harder one looks, the more one finds.* The Journal of Thoracic and Cardiovascular Surgery, 2016. **152**(4): p. 952-953.

72. Leetmaa, T., et al., *Early aortic transcatheter heart valve thrombosis: diagnostic value of contrast-enhanced multidetector computed tomography.* Circulation: Cardiovascular Interventions, 2015. **8**(4): p. e001596.

73. Toggweiler, S., et al., *Valve thrombosis 3 years after transcatheter aortic valve implantation.* International journal of cardiology, 2016. **207**: p. 122-124.

74. De Marchena, E., et al., *Thrombus formation following transcatheter aortic valve replacement.* JACC: Cardiovascular Interventions, 2015. **8**(5): p. 728-739.

75. Makkar, R.R., et al., *Possible subclinical leaflet thrombosis in bioprosthetic aortic valves.* New England Journal of Medicine, 2015. **373**(21): p. 2015-2024.

76. Brown, M.L., et al., *Early thrombosis risk in patients with biologic valves in the aortic position.* The Journal of thoracic and cardiovascular surgery, 2012. **144**(1): p. 108-111.

77. Vahidkhah, K., et al., *Blood stasis on transcatheter valve leaflets and implications for valve-in-valve leaflet thrombosis.* The Annals of thoracic surgery, 2017. **104**(3): p. 751-759.

78. Sondergaard, L., et al., *Natural history of subclinical leaflet thrombosis affecting motion in bioprosthetic aortic valves.* European heart journal, 2017. **38**(28): p. 2201-2207.

79. Bogyi, M., et al., *Subclinical leaflet thrombosis after transcatheter aortic valve replacement: a meta-analysis.* Cardiovascular Interventions, 2021. **14**(24): p. 2643-2656.

80. Weber, M., et al., *Blood-contacting biomaterials: in vitro evaluation of the hemocompatibility.* Frontiers in bioengineering and biotechnology, 2018. **6**: p. 99.

81. Hellmeier, F., et al., *Hemodynamic Evaluation of a Biological and Mechanical Aortic Valve Prosthesis Using Patient-Specific MRI-Based CFD.* Artificial Organs, 2018. **42**(1): p. 49-57.

82. Nauta, F.J.H., et al., *Computational Fluid Dynamics and Aortic Thrombus Formation Following Thoracic Endovascular Aortic Repair.* The Annals of Thoracic Surgery, 2017. **103**(6): p. 1914-1921.